2015

Investigation and Optimization of Bio-oil From Fast Pyrolysis of Brassica Carinata Meal

William Daniel Sonnek
South Dakota State University

INVESTIGATION AND OPTIMIZATION OF BIO-OIL FROM FAST PYROLYSIS OF BRASSICA CARINATA MEAL

BY

WILLIAM DANIEL SONNEK

A thesis submitted in partial fulfillment of the requirements for the

Master of Science

Major in Mechanical Engineering

South Dakota State University

2015

INVESTIGATION AND OPTIMIZATION OF BIO-OIL FROM FAST PYROLYSIS OF BRASSICA CARINATA MEAL

This thesis is approved as a creditable and independent investigation by a candidate for the Master of Science in Mechanical Engineering degree and is acceptable for meeting the thesis requirements for this degree. Acceptance of this does not imply that the conclusions reached by the candidate are necessarily the conclusions of the major department.

Gregory Michna, Ph.D.
Major Advisor/Thesis Advisor Date

Stephen Gent, Ph.D.
Co-Advisor/Thesis Advisor Date

Kurt Bassett, Ph.D.
Head, Department of Mechanical Engineering Date

Dean, Graduate School Date

To my parents: thanks for all your help.

ACKNOWLEDGEMENTS

A special thank you to my parents for encouraging me to attend graduate school and for all their help over the course of my entire educational experience.

Thanks to Jim Lawburgh, Brian Lawburgh, and Zach Parks for all their help in the lab.

Thank you to Dr. Stephen Gent and Dr. Gregory Michna for helping me through the repeated revisions of this thesis.

TABLE OF CONTENTS

ABBREVIATIONS

ACFH – Actual cubic feet per hour

ANOVA – Analysis of variance; a test used to determine if multiple sets of means are statistically different from each other.

$C_{baffling}$ – reactor baffling correction factor

cfm – cubic feet per minute

EC – Energy Content

FBR – Fluidized Bed Reactor; a reactor with a hot sand bath that pyrolizes biomass by bubbling it up through the sand with a nitrogen stream.

HVBO – High Viscosity Bio-Oil; a higher density, higher viscosity bio-oil produced through pyrolysis that is characterized by a low water content and a high energy content.

J/g – Joules per gram

KF – Karl-Fischer; the titration method used to determine water content

kJ/kg – kilojoules per kilogram

KOH – Potassium Hydroxide

LVBO – Low Viscosity Bio-Oil; a lower density, lower viscosity bio-oil produced through pyrolysis that is characterized by a high water content and allow energy content.

mg KOH/g oil – milligrams of potassium hydroxide per gram of oil

MJ/kg – megajoules per kilogram

Pa-sec – Pascal seconds, a measure of dynamic viscosity

psig – pounds per square inch, gauge pressure

r_i – inner radius of the reactor

r_o – outer radius of reactor

SCFH – Standard cubic feet per hour

TAN – Total acid number; the total number of strong acids in an oil. Usually reported by the amount of potassium hydroxide needed to neutralize the acid in the oil, e.g. mg KOH/g oil.

LIST OF FIGURES

LIST OF TABLES

LIST OF EQUATIONS

ABSTRACT

INVESTIGATION AND OPTIMIZATION OF BIO-OIL FROM FAST PYROLYSIS OF BRASSICA CARINATA MEAL

WILLIAM DANIEL SONNEK

2015

Fast pyrolysis is one method of creating bio-oil from biomass such as lignin, prairie cordgrass, and other organic commercial and industrial byproducts. In this thesis, fast pyrolysis of *Brassica carinata* meal, or simply carinata meal, was performed in an auger-type reactor. A parametric study was conducted to investigate the differences in yield, calorific, rheological, and stability property differences between the bio-oils created at five reactor temperatures and two condenser temperatures. The viscosity, water content, energy content, and acidity of the oils were measured using a rheometer, Karl-Fisher titration, a bomb calorimeter, and a titrator, respectively. The aging of the bio-oil was investigated by reevaluating these properties at 1 day, 7 days, 14 days, 28 days, and 84 days after the oil was created. Two oils were created, stratifying upon collection to produce a low-viscosity bio-oil and a high-viscosity bio-oil. The high-viscosity bio-oil was determined to be the better product. It was found that any reactor temperatures above 500°C produce bio-oils of similar composition, although with changes in yield, while high viscosity bio-oil created at 450°C had higher energy contents than the other temperatures, with an average of 29 MJ/kg versus an average of 27 MJ/kg. Condenser temperature had a significant impact on oil properties, with lower condenser temperatures showing higher energy contents and lower viscosities. In addition, the aging results of the bio-oils tested have shown insignificant changes in TAN, water content, and energy

content, while viscosity increased considerably. The best return, as characterized by the energy content per kilogram of processed biomass, is at the 600-40 reactor/condenser temperature with a return of 5.54 MJ/kg biomass input.

CHAPTER 1: INTRODUCTION

Fast pyrolysis is one method of producing bio-oil from biomass feedstocks. By using heat to thermochemically alter a biomass, the biomass can be converted to three products: char, bio-oil, and gas. These products can then be used for multiple applications. If the biomass is a byproduct of a different process, this could convert the leftover biomass into a value-added product. One source that may show some promise is the meal of *Brassica carinata*, an oilseed that can be grown in arid locations around the world. The seeds of *Brassica carinata* can be used to produce bio-oil through hexane extraction processes, but this leaves behind a meal byproduct that could be converted into a higher-value product through fast pyrolysis. This thesis will look at pyrolysis, detail the properties of carinata, and examine pyrolysis-derived carinata oil in order to test the hypothesis that carinata meal can be converted into bio-oil through fast pyrolysis.

1.1. Significance of Research and Motivation

The U.S. Department of Energy and the U.S. Department of Agriculture both support the research of renewable energy fuel sources to reduce the need for oil and gas imports, to boost the economy, and to start new domestic industries such as biorefineries [1]. Biofuels created from biomass could be potential sources for fuel, especially transportation fuel. The biomass could come from either agricultural crops specifically grown for the purpose of energy to excess or waste biomass, such as agricultural residues, yard clippings, or manure. The current use of biomass for fuel production accounts for approximately three percent of the total energy for the United States. A congressional panel, the Biomass R&D Technical Advisory Committee, is urging that biomass-derived

energy should account for 30 percent of the total energy for the US by year 2030 [1]. It is possible that bio-oil derived from pyrolysis could help account for some of that production.

The primary aim of this particular research, however, is to create a value-added product from meal byproduct. Carinata is already used for bio-diesel production via cold pressing or hexane extraction of its oil. These methods leave behind a waste meal. The meal can be used as a protein supplement for cattle, but it can only be fed to them in small amounts; carinata contains glucosinolates, which are poisonous to cattle. [2-5]. Producing a bio-oil that could be used for other applications would create a value-added product from this otherwise low value byproduct.

1.2. Research Objectives

In this thesis, the objectives are to determine:

1. the possibility of producing bio-oil from *Brassica carinata* meal,
2. the characteristics of the bio-oil produced,
3. the characteristics of the bio-oil as it ages over time,
4. the comparisons between the pyrolysis-created oil from *Brassica carinata* meals and other pyrolysis-created oils.

1.3. Organization of Thesis

This thesis will first review current literature to explain pyrolysis, analyze trends, and formulate a hypothesis. Then, the methodology will be explained and the design of

experiments presented. The results will be presented and discussed. Conclusions and recommendations for future work will then follow.

CHAPTER 2: REVIEW OF CURRENT LITERATURE

In this chapter, the biomass used in this research will be reviewed. In addition, the pyrolysis process will be assessed and compared to other biomass conversion processes, and its strengths and weaknesses detailed. The methods for characterizing bio-oils will be reviewed and current trends for state-of-the-art research detailed. Finally, reactor types will be examined. This chapter will allow for the formulation of the hypothesis used in this research.

2.1. *Brassica carinata*

Cardone et al. [6] notes that *Brassica carinata*, also referred to as *B. carinata* or simply carinata, can be grown in conditions that would be largely unsuitable for more common oilseeds. Since carinata can be grown in clay-type and sandy-type soil and in a semi-arid climate, these otherwise unproductive locales could be used to produce a renewable biofuel [7]. This would not then put a strain on the production of foodstuffs; unlike the production of corn for ethanol, carinata would not take good fields out of food production. Carinata oil produced from hexane extraction or cold pressing also has desirable characteristics that would make it suitable for biodiesel, such as a low total acid number (TAN) and low water content [6]. A relatively high energy density is also present [6]. Carinata-derived biodiesel is reported to be relatively stable with regards to acid content and viscosity [8] and has been the subject of pilot plant studies where the quality of the produced biodiesel met European standards for fuel [9]. Table 2.1 shows some of the comparisons between the preliminary carinata biodiesel and diesel, as well as the Italian Organization for Standardization (UNI) standards for diesel.

Table 2.1: A comparative analysis of B. Carinata biodiesel, commercial Diesel-Bi(r), and Italian standards for biodiesel [6]

Properties	*B. carinata* biodiesel	Diesel-Bi®	UNI 10946 standards	Test method
Methyl ester content (wt%)	98.27	98.24	>96.5	prEN 14103
Density (kg/m^3) at 15C	879	883	860-900	UNI EN ISO 3675 and 12185
Viscosity (mm^2/sec) at 40C	4.5	4.5	3.5-5.0	UNI EN ISO 3104
Flammable point (C)	>120	>120	>120	ISO/CD 3679
Sulfur (mg/kg)	<10	<10	<10	EN 24260
Conradson carbonaceous residue (wt%)	0.09	0.12	<0.3	UNI EN ISO 10370
Cetane number	52	53	>51	EN ISO 5165
Sulfated ash content (wt%)	<0.01	0.01	<0.02	ISO 3987
Water (mg/kg)	465	312	<500	prEN 12937:99
Acidity (mg KOH/g)	0.08	0.49	<0.5	prEN 14104
Iodine number (g I2/100 g)	128	115	<120	prEN 14111
Methyl ester of linolenic acid (wt%)	13.0	9.2	<12.0	prEN 14103
Methanol (mg/kg)	50	1100	<2000	prEN 14110
Bound glycerol				
Monoglycerides (wt%)	0.53	0.49	<0.8	prEN 14105
Diglycerides (wt%)	0.13	0.17	<0.2	
Triglycerides (wt%)	0.07	0.09	<0.2	
Free glycerol (wt%)	38	100	<200	prEN 14105

In addition, Applied Research Associates, Inc. (ARA) has been experimenting with processed carinata bio-oil as a possible drop-in jet fuel, something chemically similar to jet fuel that could be used without any mixing [10]. Studies suggest that, if the oilseed can be processed, carinata will grow well and in enough quantities to be a viable biofuel product [11].

As mentioned before, the specific source of carinata feedstock used in this research is the byproduct meal left over from a vegetable oil extraction process utilizing hexane solvent extraction. This can be used for production of pyrolysis oil. After this

meal undergoes pyrolysis, the only byproducts are char and nitrogen gas, the latter of which could theoretically be recycled back into the pyrolysis stream or vented to the atmosphere [12]. This char could be used as a fertilizer substitute or soil amendment [13, 14].

Carinata meal can be processed after the initial oil extraction as received, or it can be milled and/or dried. Since Harris et al. [15] reported a greater degree of success with milled and dried carinata in a fluidized bed reactor (FBR), the carinata used in this thesis was also milled and dried. Table 2.2 shows some of the properties of the carinata meal.

Table 2.2: Physical properties of carinata as reported by Harris et al. [15]

Properties	Feedstock As Received	Feedstock After Milling and Drying
Avg Particle Length (mm)	1.38	0.52
Moisture Content (dry basis)	10%	0
Calorific Value (MJ/kg)	17.7	19.5

In addition, Harris et al. [15] performed initial comparisons of carinata meal oil produced through pyrolysis versus four other types of biomass, showing that carinata produced similar results and noting its viability as a source for pyrolysis. Table 2.3 shows the comparison of results.

All energy content values fell between 22 and32 MJ/kg. Grasses showed considerably lower energy content than the byproduct meal from carinata and camelina. Lignin, another byproduct (this one from the paper-making process), also showed high energy contents. The grasses and camelina also had high acid contents, while the water contents ranged between 30% and 6.6%, with no value being reported for camelina.

Table 2.3: Comparison of pyrolysis oil from five different feedstocks [15]

Feedstock Species	Energy Content (MJ/kg)	Total Acid Number (mg KOH/g oil)	Water Content (%)
Brassica carinata	26.7	34.6	16.5
Camelina sativa	26.2	93.03	N/A*
Prairie cordgrass	21-23.5	86.9	30.2
Lignin	29-32	35.8	6.6
Switchgrass	22-25	119	6.7

*A leak in the condensers invalidated this measurement.

2.2. Conversion of Biomass into Value-Added Products and Fuels

There are three primary pathways for the conversion of biofuels and bioproducts from agricultural residues. Mechanical conversion is mainly used to squeeze product out of biomass, cold pressing being one such example. Biochemical conversion utilizes fermentation to chemically degrade feedstock into bio-based products, the most common example being ethanol. Thermochemical conversion, by contrast, relies on chemical reactions based on carefully controlled temperatures and/or pressures to convert the feedstock into a preliminary oil that can then be converted into biofuels and bioproducts. Pyrolysis falls into this latter category [16]. Figure 2.1 shows some conversion methods, with their output and potential markets, while Figure 2.2 focuses on thermal conversion methods and their markets.

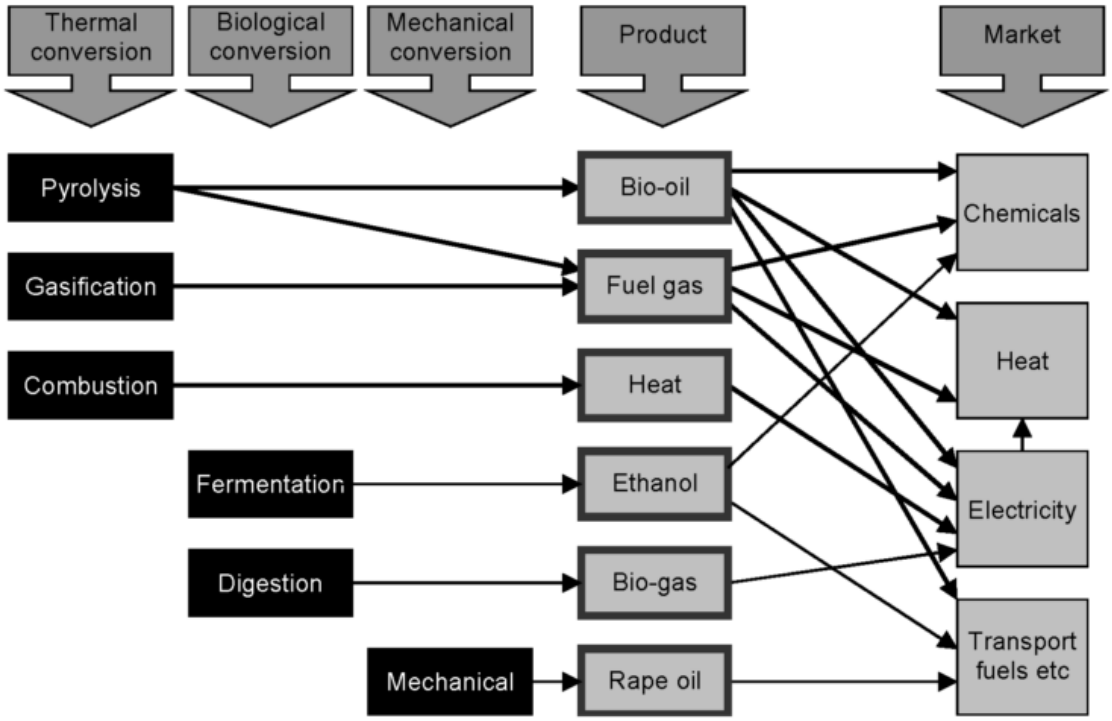

Figure 2.1: Conversion processes, products, and applications [16]

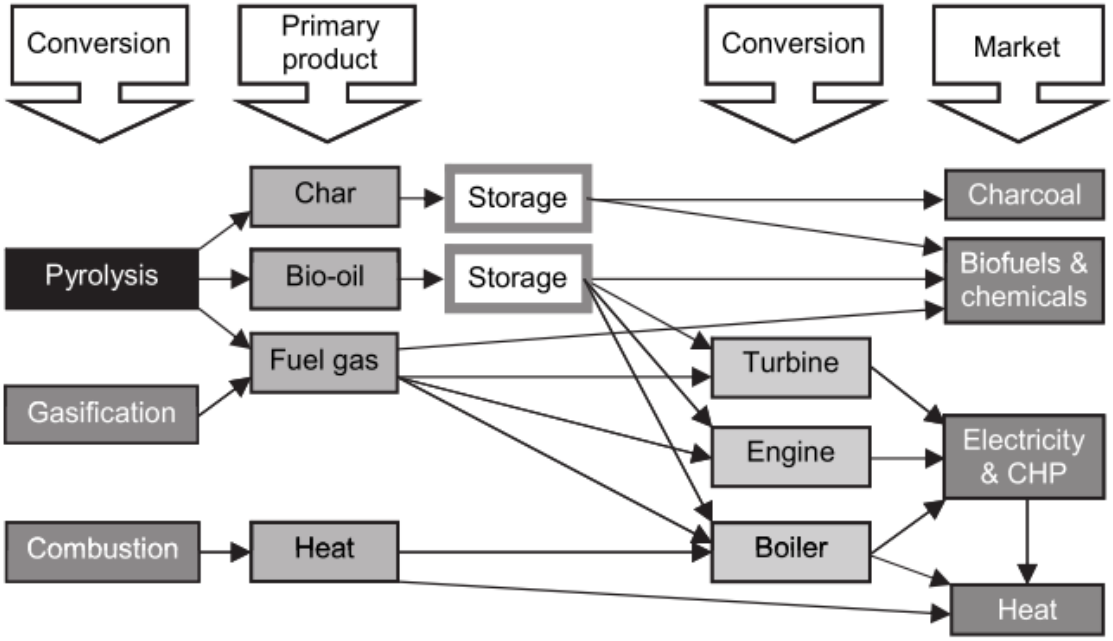

Figure 2.2: Products from thermal biomass conversion [17]

Biomass feedstock conversions have primarily found applications in ethanol production, e.g. corn via biochemical conversions. The most common example is ethanol production. Fast pyrolysis of farm residue biomass has only recently been studied, with some reported results of nonfood oilseed meal undergoing fast pyrolysis [18-20].

Using pyrolysis to convert oilseed meals into a higher-value, more energy dense and storable liquid transportation fuel would allow oilseed meal processors to create a domestic, readily available source of energy for transportation applications. Even if bio-oil cannot be produced from the pyrolysis oil made by pyrolysis, there are other markets for pyrolysis oil.

Czernik and Bridgwater [21] studied the applications of bio-oil produced from fast pyrolysis; potential markets include combustion in burner/furnace and burner/boiler systems, upgrading to transport fuels (which they noted was not economically feasible as yet), and chemical production. The last market was the most promising; chemicals produced from whole bio-oil include carboxylic acids and phenols which can easily react with lime to form calcium salts and phenates. A product has already been formed to capture SO_x emissions from coal combustors in power plants. Chemicals produced from fractionation of pyrolysis bio-oil include low-molecular-weight aldehydes that are effective meat browning agents. Biomass-derived de-icers have also been developed. There could also be chemical compounds in the bio-oil itself. They reported that "Levoglucosan…and levoglucosenone…are not typical components of bio-oil produced for fuel application but can be generated with high yields by a similar pyrolysis processes from demineralized cellulose or biomass" [21].

2.3. Pyrolysis and Bio-Oil Production

Pyrolysis is, by definition, the thermochemical decomposition of biomass at temperatures between 400 and 650°C in the absence of oxygen. It is typically classified as either “fast” or “slow” pyrolysis. Biomass is fed into a reactor along with an inert carrier gas. The inert gas, usually nitrogen, prevents combustion in the reactor, which would result if any oxygen were present. The reactor heats the material and thermally degrades it, producing char, synthesis gas, and condensable vapors. The vapors can then be condensed to collect bio-oil. The parameters affecting pyrolysis are the reactor temperature, the biomass feed rate, the solids residence time (the length of time the solids spend in the reactor), the gas residence time (the length of time the gases spend in the reactor), and the condenser temperature [12]. Pyrolysis reactions are complex and not entirely understood as of yet [18], although Bridgwater reports that pyrolysis utilizes “thermal degradation by primary reactions, giving gas, vapours and aerosols that can be condensed to liquid and char. The vapours and aerosols may undergo secondary reactions and either form lighter organics through cracking, and/or char through repolymerisation reactions.” [12]

Fast pyrolysis is seen as a promising method for converting oilseed meals into liquid bio-oil. It takes place at moderate temperatures, typically near 500^{o}C with rapid heating rates from 10 to over 100°C/s and with a short hot vapor residence time in the order of seconds. Bio-oil yields around 50-60% and as high as 75% have been reported for some reactors [12, 17]. Due to the speed at with the reaction takes place, the biomass must first be reduced to a particle size of two millimeters or smaller in diameter [12, 18, 22, 23]. Slow pyrolysis takes place at low to moderate temperatures (400-500^{o}C) with

slow heating rates of 0.1 to 1.0°C/s and at longer vapor residence times measured in minutes or hours. Methanol and nearly equal quantities of char, gas and liquid have been produced with this method, versus the 50-75% liquid yield that can be obtained from fast pyrolysis [17, 18]. Bridgwater reported that the oil ranged from 15% water content by weight to 30-50% depending on the feed material and how it was produced [17]. Slow pyrolysis has been used for the production of charcoal, with the liquid oil usually incinerated as waste. Fast pyrolysis has liquid oil as its desired product, with char usually discarded, although some research suggests it could be used as a soil supplement [12, 13].

Slow pyrolysis is not to be confused with gasification or torrefaction. Gasification operates at high temperatures (greater than 800^{o}C) and at long vapor residence times, producing syngas (a mixture of carbon monoxide, hydrogen, and methane). Torrefaction operates at lower temperatures, around 300^{o}C, and produces solid biochar and volatile off-gases.

Pyrolysis has an overall lower efficiency compared to other biomass conversion processes such as combustion, which produces an immediate product, heat, and converts more of the available energy into a form that can be readily used. Pyrolysis produces a liquid bio-oil that must be upgraded or altered before it can be used for fuel, chemicals, or other products. However, since liquids are easier to pump, transport, store, and use than solids, and since liquids have a distinct energy density advantage over gases, they are more desirable for use in storage and processes [12, 17].

2.4. Characterizing Bio-Oils

Bio-oils tend to be characterized by their energy content, total acid number, water content, and viscosity. Many authors, including Bridgwater [17], Bridgwater and Coulson [12], Alcala and Bridgwater [24], Shen et al. [22], Grioui et al. [25], Harris et al. [15], and others have used some combination of the four to characterize pyrolysis-produced bio-oil. Viscosity is reported as either kinematic or dynamic viscosity. All four of these methods are also used to characterize transportation fuel [6], so they are often used as a benchmark comparison to analyze differences between pyrolysis oil and bio-diesel or commercial diesel.

In addition, elemental analysis [25, 26] or even mass spectroscopy [27] can be reported for the bio-oil. The way the bio-oil ages, or changes characteristics with time, can also be reported. Hilten and Das [28] noted that viscosity changed during their accelerated aging of their pyrolysis-produced bio-oil derived from pine pellets and peanut hulls, while Grioui et al [25] saw aging increase the viscosity of their almond-shell-derived oil considerably over five years of storage at room temperature.

2.5. Trends on Bio-Oils Produced from Feedstocks

The composition of pyrolysis products is influenced by how the reaction is controlled, particularly with pyrolysis temperature and residence time. Bridgwater [17] looked at the composition of the products of two types of fast pyrolysis of a woody biomass and compared them to other forms of thermal biomass conversion methods (Table 2.4).

Table 2.4: Product Compositions for Fast Pyrolysis versus Other Biomass Conversion Methods [17]

	Temp	Gas Res Time	Liquid	Solid	Gas
Fast pyrolysis	~500°C	~1 sec	75%	12% char	13%
Fast pyrolysis	~500°C	10-30 sec	50% in 2 components	25% char	25%
Carbonization	~400°C	Days	30%	35% char	35%
Gasification	~750-900°C		5%	10% char	85%
Torrefaction	~290°C	Solid residence time 10-60min	0%	80% solid	20%

Table 2.4 shows what can be expected for the pyrolytic conversion of carinata. If the gas flow rate can be set to a rate that results in less than or equal to a one-second gas residence time, a liquid yield of as much as 75% can be expected. Harris et al. [15] only collected one type of oil from their experiments with a gas residence time of 3 seconds. If the flow rate is lower, then it would appear likely that a liquid yield of 50% in two different forms could be collected [17, 29], since short gas residence times are more conducive to forming condensable liquids, while longer times produce a greater percentage of non-condensable gases [17].

Pyrolysis is already being considered in industry. Certain renewable oil companies, such as Renewable Oil International® LLC [30], are considering the possibility of converting biomass to oil before shipment. Wood chips, for example, have a low energy density compared to their associated pyrolysis-derived bio-oil. Converting

wood into bio-oil before shipment would cut down on handling costs and contamination, such as dust or noise that is commonly associated with transporting wood resources [30]. Bridgwater [31] conducted a techno-economic comparison of this particular process for power generation, concluding:

> "[T]he fast pyrolysis and diesel engine system has great potential to generate electricity at a profit in the long term, and at a lower cost than any other biomass to electricity system at small scale. This future viability can only be achieved through the construction of early plant [sic] that could, in the short term, be more expensive than the combustion alternative. Profitability in the short term can best be achieved by exploiting niches in the market place and specific features of fast pyrolysis." [31]

Some of these niche market sections are shown in Figure 2.3. Depending on the processing methods, several different products can be derived from pyrolysis oils.

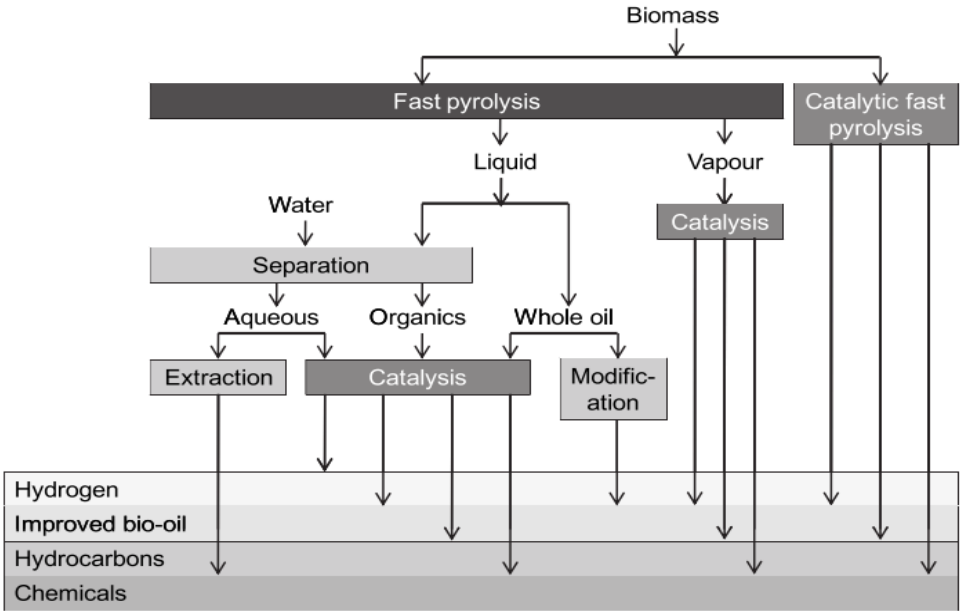

Figure 2.3: Potential Markets for Products for Pyrolysis [17]

Rape oil is already being considered as a biofuel, although there are many improvements that need to be made in order for it to be a competitive fuel source. Examples of hurdles that need to be overcome are the energy-input-to-energy-derived-from-biomass ratio, the bio-oil compatibility with current filters, and waste products associated with the production [32].

The carinata meal used in this research is the byproduct from a hexane solvent extraction of vegetable oil. The meal byproduct currently has little or no use, but it could be converted into a higher-value bio-oil or renewable fuel source. Some successful pyrolysis bio-oil conversions have been performed on other waste products, such as sawdust, sugarcane straw, chicken litter, and cashew nut shells [29, 33], lignin from paper-making processes [34, 35], mallee eucalypts (a woody product) [26], corn stalks

[33, 36], wood and bark [37], almond shells [25], and switchgrass and reed canary grass [23], among others.

Pyrolysis oils are low-grade fuels when compared to transportation fuels, with multiple components, high water, acid, viscosity, and oxygen contents, and lower heating values with poor ignition properties [38]. Pyrolysis oils have been blended with biodiesel in an attempt to overcome the deficiencies present, yielding some stable oil with higher heating values as compared the pyrolysis oil but lower than the pure biodiesel [24].

2.6. Catalyst

The goal of catalyst is to remove oxygen from the oil and to catalytically crack the high molecular weight compounds [39]. This also reduces total acids in the oil, as well as condensing more of the aromatics in the pyrolysis vapors; however, more non-condensable gas is produced, resulting in less oil collected [39]. Zeolite catalysts are the most commonly used for this type of oil-producing fast pyrolysis, due to its success and due to the fact that it can be regenerated to a degree, with the catalyst losing effectiveness with successive regenerations [40]. The regeneration process begins degrading the catalyst to a certain extent[41]. Mihalcik et al. [39] tested nine different types of zeolite catalyst with eight different feedstocks to determine which was preferable for pyrolysis production and found that H-ZSM-5 catalyst with a SiO_2/Al_2O_3 ratio of 23 provided the best results, balancing the reduction of oxygenates with the production of condensable aromatics. Mihalcik et al. used a biomass/catalyst ratio of 1:5 to avoid determining the deactivation of the catalyst.

2.7. Auger Reactor Types

There are several reactors that can be used for pyrolysis, such as the ablative reactor, the circulating fluid bed reactor, the entrained flow reactor, and the rotating cone reactor, among others [42]. The two reactors at this facility are the fluidized bed reactor (FBR) and the auger reactor.

2.7.1. Fluidized bed reactor

The FBR operates by entraining biomass in an inert gas and bubbling it through a heated sand bath. The sand provides a nucleation point for the pyrolysis reaction to take place. The char remains in the sand while the pyrolysis vapors are driven by the carrier gas to the condensers, where the oil is condensed and collected. An electro-static precipitator (ESP) can also be hooked up to the system. It operates by inducing a charge in the vapor particles and driving them to the oppositely-charged walls of the precipitator; in essence, using electricity to force the vapors to precipitate so that oil can be collected [17]. The oil is collected by removing the condensers and/or precipitator and removing the oil by manually scraping the inner surface.

The advantage to the FBR is its precision; temperatures can be controlled to within ±1°C, and results can be repeated to a great degree of precision. That repeatability and precision comes at a cost, however; the FBR available for this research cannot make more than 60 mL of oil at any one time and must be thoroughly disassembled and cleaned between each run in a process that takes several hours. The FBR is the most common in pyrolysis research, and attempts at modeling the reactions and behavior of it have been moderately successful [34, 43].

2.7.2. Auger reactor

The auger reactor differs from the FBR in the reaction chamber. Instead of heated sand, the walls of the reactor are heated with ceramic heaters and the biomass is driven through the reactor with an auger. The vapors produced are carried to the condensers by the nitrogen stream, while the auger carries the solids to a containment vessel for collection. The auger reactor can typically produce larger quantities of oil than the FBR.

2.8. Summary of Literature Review

The primary thrust of this research is to investigate the production of a value-added product from a byproduct of oil processing. Fast pyrolysis seems to be a good choice of method due to the successful conversions of multiple other feedstocks and initial success with samples of carinata meal. It also has the potential to create a value-added product, since several potential markets exist for improved bio-oil, hydrocarbons, and chemicals; these cover heat, electricity, chemicals, and fuels. Some products have already been created, such as meat browning agents and de-icers, and some markets exist in the heat industry for combusting bio-oils for fuel. Another advantage of bio-oil, as opposed to raw biomass, is ease of transportation; liquids are typically easier to transport than solids.

Pyrolysis itself is the thermochemical decomposition of biomass at temperatures between 400 and 650°C in the absence of oxygen. Fast pyrolysis produces the most oil; it operates near 500°C with rapid heating rates that range from 10°C/s to over 100°C/s. In order to characterize the bio-oil, the energy content, total acid number, water content, and

viscosity are good benchmark values for comparison to other types of pyrolysis oils as well as other fuels. Yields around 50% can be expected [17, 33].

There has been a considerable amount of research into markets for pyrolysis oil. Combustion, upgrading to transport fuels, and chemical production are the top three markets so far. However, current pyrolysis technology is difficult to model. The complicated reactions within the process make it more efficient to map results experimentally for individual feedstock/reactor combinations. Some success has been reported in modeling fluidized bed reactors using kinematic properties, however [43].

The pyrolysis reactors face limitations in efficiency. Other biomass conversion processes have greater efficiency than pyrolysis; combustion, for instance, produces a product, heat, that can be immediately used. While pyrolysis oils can be directed towards multiple markets, the oils must first go through substantial post-processing and refining in order to prepare them. When compared to other forms of biomass conversion products, this can be a substantial hurtle to overcome; ethanol from fermentation, for instance, can be ready to sell with little, if any, refinement.

These limitations could be alleviated with further study and optimization of processing methods; they are not enough to fatally cripple the research of pyrolysis oils. The next chapter explains the hypothesis and the experiments which explore the possibilities of carinata oil in order to provide a good picture of its properties.

CHAPTER 3: HYPOTHESIS AND EXPERIMENTAL STUDY

3.1 Hypothesis

The hypothesis that was tested in this research was that carinata meal will produce a bio-oil through fast pyrolysis which, due to the abilities of the auger unit, will have a yield of 50% liquid in two phases varying with reactor and condenser temperature [15, 17]. The produced bio-oil will have an energy content that ranges between 22-30 MJ/kg [15-17], and the viscosity of the bio-oil will increase over time [25, 28].

3.2. Production of Bio-Oil

3.2.1. Feedstock preparation

The feedstock used was the same as the feedstock used in the Harris et al. report [15]. The feedstock was received as a coarse meal. In order to prepare it for the auger reactor, the feedstock was first ground with a hammer mill into a fine meal before being dried in an oven at 200°F with stirring taking place every hour to prevent clumping. To determine when it was thoroughly dried, the mass was weighed every hour. When the mass remained constant for three hours, the feedstock was deemed to be thoroughly dried. It was then stored in an airtight container until used. The maximum storage time was 30 days. Table 3.1 shows the sizes of the various stages of feedstock preparation.

Table 3.1: Particle distributions of the feedstock [15]

Preparation of carinata meal	Largest Particle Length (mm)	Smallest Particle Length (mm)	Average Measured Length (mm)
As Received, Undried	1.85	0.12	0.73
Ground, Undried	1.13	0.11	0.54
Ground, Dried	0.54	0.07	0.21

3.2.2. Experimental Apparatus—Auger Reactor

The auger reactor operates by feeding biomass into an auger, which then drives the biomass through a horizontal heated cylindrical reactor. The reactor is heated with electrical ceramic heaters placed on the outside walls of the reactor. As the auger drives the biomass forward, the pyrolysis reaction takes place on the heated walls of the reactor. The pyrolysis vapors are driven forward by an inert gas flowing through the reactor, in this case nitrogen, to the condensers, of which there are four in series in a condenser train. The char continues to be driven to the far end of the reactor and drops out into a sealed collection bin for removal later. Removal during pyrolysis would result in air, with its accompanying oxygen, entering the reactor and causing combustion [37].

Since the condensers are too large to deconstruct and do not provide any method of easy cleaning, collection jars are sealed to their bottom valves and the valves then opened for collection. Due to the viscosity of the oil, the collection time for the oil is 20 hours to allow it to drain into the collection jars.

The advantage to the auger reactor is its ability to be run with a minimum of preparation and its ability to make large quantities of oil. The cost to that is its relative imprecision; the temperature can be controlled to ±10°C, at best, and oil production yields between repeated batches can vary as much as 15%. In addition, the reactor cannot cope with the high nitrogen flow rate needed to create a single-component carinata oil. However, all oil properties remain similar for similar tests. Since large quantities of oil will need to be produced, not just for this thesis but for future analysis, the auger reactor will be used for this study. Auger reactors are not as prevalent as FBRs due to the reduced surface area available for pyrolysis reactions to take place, which allows the FBR

to have a higher heat transfer rate [43]. Still, auger reactors have seen some success, due to their relative ease of operation compared to FBRs, and have been used on corn stalks [36] and wood and bark [37]. Figure 3.2 is a schematic of the auger reactor, and Figure 3.1 is a picture of the auger reactor used in this study.

Figure 3.1: Auger Reactor

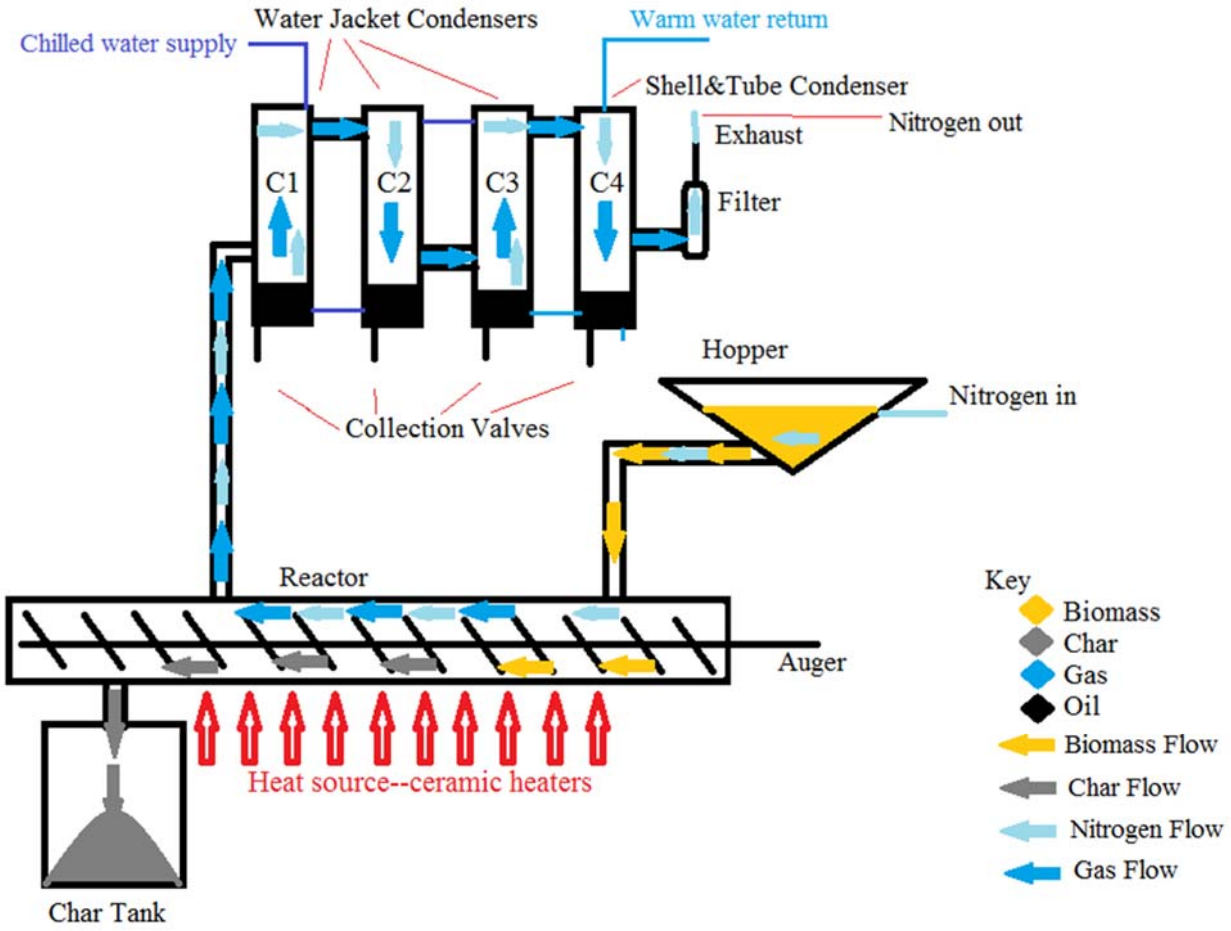

Figure 3.2: Schematic of the Auger Reactor

3.2.3. Design of experiments

First, several runs were made in order to study the repeatability of the reactor. Once the repeatability was determined, the gas flow rate and the solids residence time were changed individually in order to remove them from the main experiment. The results from these preliminary runs were measured by yield and energy content. When the titrator was available, water content were also measured with the Karl-Fisher method.

Second, the main experimental runs were conducted to determine the effect of reactor temperature and condenser temperature on the production of bio-oil, with a one-run catalyst comparison. Table 3.2 and Table 3.3 show the independent and dependent variables for this study and Table 3.4 shows the runs that were conducted.

Table 3.2: Experimental Variables

Independent Variables			
Reactor Temp. (C)	Condenser Temp (C)	Age of Oil (Days)	Dependent Variables
400	20	1	Yield (Mass Fraction)
450	40	7	Water Content (%)
500		14	Energy Content (J/g)
550		28	TAN (mg KOH/g oil)
600		84	Dynamic Viscosity (Pa-sec)

Using the variable information from above, parameters were set as follows in Table 3.3.

Table 3.3: Independent Variable Constants

Biomass Per Run:	1.5 kg
Nitrogen Inlet Pressure:	35 psi
Nitrogen Flow Rate:	6 cfm
Mass Feed Rate:	3 kg/hr
Collection Time:	Overnight*

Solids Residence Time Per Temperature		
Solids Residence Time	Reactor Temperature	Dial Setting
38 seconds	400°C	1.5
24 seconds	450°C	1.75
14 seconds	500°C	2.5
14 seconds	550°C	2.5
12 seconds	600°C	2.75

* A nominal 20-hour collection time was used. Tests usually finished at noon with the weighing taking place at 8 A.M. the following morning

Table 3.4: Experimental Program

Run	Reactor	Condenser	Catalyst
1	400 C	20	No
2	450 C	20	No
3	500 C	20	No
4	550 C	20	No
5	600 C	20	No
6	450 C	40	No
7	500 C	40	No
8	550 C	40	No
9	600 C	40	No
10	500 C	40	10:1*

*10:1 biomass/catalyst ratio

For ease of referral, each test will be referred to by the reactor-condenser temperature: e.g. 500-20 or 600-40. When referring specifically to the low viscosity bio-oil (LVBO) or the high viscosity bio-oil (HVBO), an H or L was added to the end of the

test name; e.g. 450-20H. The catalyst run had a “Cat” added to the end of the name (500-40Cat or 500-40LCat).

This research used H-ZSM-5 catalyst with a SiO_2/Al_2O_3 ratio of 23. Since this thesis will be primarily focused on the effects reactor and condenser temperature on the carinata, this is only a one-run brief comparison with a 1:10 biomass/catalyst ratio.

The dependent variables of yield, energy content, total acid number (TAN), and dynamic viscosity were measured one day after each run was completed. Each of the tests for TAN, water content, and energy content was run three times to collect a standard deviation for each test.

Those four tests were also repeated 7 days, 14 days, 28 days, and 84 days after the run was completed to test the effects of aging on the oil, with all points being taken within ±3 days of the first three times and ±9 days for the last time.

3.3. Analysis of Bio-Oil

3.3.1. Bio-oil preparation

The bio-oil was placed into 30 mL sample vials and stored on shelves at room temperature out of direct sunlight. As the oil aged and increased in viscosity, a few runs were placed in hot water baths to decrease the viscosity enough to draw a sample. Samples were measured dropwise with 1 mL syringes.

3.3.2. Mass measurement

The mass of the feedstock, oil, and char samples were measured with a Mainstays Digital Scale with an uncertainty of 1.0 gram. Masses used in the energy content, TAN,

and water content measurements using a Denver Instruments laboratory scale with a uncertainty of 0.0001 gram (0.1 mg).

3.3.3.. Energy content

Energy content was measured with an IKA C5003 bomb calorimeter, calibrated using a benzoic acid standard. The uncertainty of the experimental apparatus is <0.2% [44]. Experimental and procedural uncertainty was determined to be ±210 kJ/kg.

Oil samples were combined with a mineral oil to enhance combustion, due to the poor ignition properties of pyrolysis oils [38]. The mineral oil had an energy content of 46.3 MJ/kg, and its energy content was removed from the final energy content value to determine the energy content of the oil. The mineral oil used was Vi-Jon Mineral Oil, U.S.P.

3.3.4. Water content

Water content was measured using the Karl-Fischer titration method with a Metrohm 907 Titrando. The software used was Metrohm Tiamo version 2.8. The titrant used was HYDRANAL-Composite 5, and the solvent was HYDRANAL-Liposolver CM. The combined uncertainty for the procedure and machine was determined to be <3.5%.

3.3.5. Total acid number

The total acid number was measured with a Metrohm 907 Titrando. The software used was Metrohm Tiamo version 2.8. The titration method utilized 0.01N potassium hydroxide in isopropanol as the titrant and a solvent that was 50% toluene, 45% 2-propanol and 5% deionized, ultra-filtered (DIUF) water. Total uncertainty for the method and machine was determined to be ±2 mg KOH/g oil.

3.3.6. Dynamic viscosity

The dynamic viscosity was measured with an AR 200 EX Rheometer, calibrated with a mineral oil standard obtained from the Canon Instrument Company [45]. Data were averaged for 30 shear points ranging from a head speed of 1 rad/sec to 1000 rad/sec for data measured at -5^{o}C, 25^{o}C, 50^{o}C, and 80^{o}C, then averaged across the temperatures for a final average viscosity. Since two different oils, a low viscosity bio-oil (LVBO) and a high viscosity bio-oil (HVBO), were collected and measured, all four temperatures were measured for each oil; however the LVBO was only reported at -5^{o}C, 25^{o}C, and 50^{o}C due to boiling at 80^{o}C, and HVBO was reported at 25^{o}C, 50^{o}C, and 80^{o}C due to excessive thickening causing it to become too viscous for the rheometer at -5^{o}C.

3.3.7. Statistical analysis

Minitab 17 was used to perform statistical analyses on the data collected. Since multiple means were being compared (each run had three associated tests—water content, energy content, and total acid number—that were each performed three times), the statistical method of analysis of variance, or ANOVA, was most commonly used. ANOVA determines if there was a significant difference between means at a specific confidence interval; in this case, a 95% confidence interval. Since ANOVA merely states whether there is or is not a statistically significant difference, but not what that difference actually was, this test was coupled with the Fisher test to determine which sets of means differed from each other. Yield and viscosity could not be tested with these methods due to the lack of sufficient runs to make that determination.

CHAPTER 4: RESULTS, INTERPRETATION, AND DISCUSSION

Once the runs were completed, the data were analyzed with Excel for the tables and some of the graphical presentations and Minitab for the statistical tests. The main effects of reactor and condenser temperatures were studied on the basis of how they affected the energy content, water content, total acid number, and viscosity. Aging and catalyst were also evaluated.

4.1. Tabular and Graphical Presentations of Data Collected

4.1.1. Variable determination and removal

The solids residence time and gas residence time of the reactor were both assessed to determine the most optimal reactor operating conditions. A repeatability study was also conducted, to determine the precision of the reactor yield and to determine variability in yield data.

4.1.1.1. Repeatability study setup

The auger operating parameters were set and held constant for the duration of the study. The reactor temperature was set to 500°C and the condenser set to 40°C, since pyrolysis results are usually best near those temperatures [12]. The gas residence time was determined by the nitrogen flow; the nitrogen flow was set to 6 cfm at room temperature. This was the lowest setting of which the reactor is capable and it was chosen to conserve nitrogen and to give the vapor the maximum amount of time possible in the condenser train. The auger speed, which determines how fast the biomass moves through the reactor, was set to 20 seconds residence time. The biomass feed rate was set to 3

kg/hr. The mass of the carinata that was used was 1.5 kg per test run. Since neither the bomb calorimeter nor the titrator were available for these runs, the yield was the only result measured. The collection time was set for two hours, with plates then placed underneath to see if any more oil fell out over the course of the next few days.

4.1.1.2. Repeatability study results

Condenser 1 (C1) collected the most oil out of all four condensers, full orders of magnitude above the other three. The other three collected a maximum of 60 grams of oil, while C1 collected between 410 and 660 grams of oil each run. The oil that was collected from C1 separated into two components: a more viscous oil on the bottom, referred to as High Viscosity Bio-Oil (HVBO); and a less viscous oil on the top, referred to as Low Viscosity Bio-Oil (LVBO). The less viscous oil was decanted and measured separately. Overnight collection yielded an additional 30-70 grams of oil; past that, future days only yielded negligible gains of 1-5 grams total. Figure 4.1 shows the oil collection results. There is a slight downwards trend that is hypothesized to have come from improvements in the carinata drying methods. The HVBO and the LVBO collect less water when the carinata is drier.

Figure 4.1: Repeatability Study Collection Results

The LVBO is the majority of the oil collection. Condensers C2 through C4 did not collect any LVBO oil during this study. An oil spill due to operator error on C1 invalidated the C1 collection for run 1, although it was estimated that the C1 total oil collection was between 600g and 650g.

4.1.1.3. Solids residence time study setup

A study of the solids residence time, as controlled by the auger speed, was made to determine its effects on the bio-oil. The reactor temperature was set to 500°C and the condenser set to 40°C. The gas residence time, as determined by the nitrogen flow, was set to 11 seconds of residence time in the reactor to conserve nitrogen and to give the vapor the maximum amount of time possible in the condenser train. The solids residence times tested were 38, 14, 12, and 10 seconds. The biomass feed rate was set to 3 kg/hr.

The mass of the carinata that was used was 1.5 kg per test run. Yield, energy content, and water content were measured. The collection time was set for overnight collection.

4.1.1.4. Solids residence time study results

A residence time of 14 seconds was to be the best time to optimize yield without damaging the auger for the 500°C reactor temperature. Repeated jams occurred, where the auger froze in place and refused to turn until a higher speed, with a corresponding increase in power, was implemented. The jams happened at the 38 second residence time, and incomplete pyrolysis was evident at 10 and 12 second residence times. Energy content and water content differences were negligible across the various runs. Table 4.1 shows the results of the experiment.

Table 4.1: Solids Residence Time Study Results

Auger Speed	Solid Residence Time (sec)	Oil Yield (mass fraction)	Char Yield (mass fraction)	LVBO Energy Content (kJ/kg)	HVBO Energy Content (kJ/kg)	LVBO Water Content (%)	HVBO Water Content (%)
1.5	38	0.44	0.41	7900	27400	63.19	11.41
2.5	15	0.37	0.48	7900	27300	63.24	11.64
2.75	12	0.31	0.56	7900	27500	65.32	11.09
3	10	0.33	0.55	7500	27200	65.25	12.58

The general trend was found to be higher solid residence times gave better yields. A few additional runs were made at reactor temperatures of 400°C, 450°C, 500°C, 550°C, and 600°C to study the behavior of the auger at the other temperatures. It was found that the solids residence time had to be varied, and faster times applied to the higher temperatures, in order to prevent auger jamming. Table 4.2 shows the best solids residence time for each temperature.

Table 4.2: Optimization of Solids Residence Time for the Auger Reactor

Solids Residence Time Per Temperature		
Solids Residence Time	Reactor Temperature	Dial Setting
38 seconds	400°C	1.5
24 seconds	450°C	1.75
14 seconds	500°C	2.5
14 seconds	550°C	2.5
12 seconds	600°C	2.75

4.1.1.5. Gas flow rate study

A study of the gas residence time, as controlled by the nitrogen flow rate, was made to determine its effects on the bio-oil. The reactor temperature was set to 500°C and the condenser set to 40°C. The auger speed was set at 2.5, corresponding to a 14 second residence time. The biomass feed rate was set to 3 kg/hr. The mass of the carinata meal that was used was 1.5 kg per test run. Yield and energy content were measured. The collection time was set for overnight collection.

Gas flow rate was varied by the upstream rotameter at room temperature, at 6 cfm, 10 cfm, and 20 cfm. Since the operating temperature of the reactor was considerably different than the 20°C at the inlet, a conversion had to be calculated to determine the gas residence time inside the reactor. The rotameters at the nitrogen inlet read in $SCFH_{Air}$. Using the law of perfect gasses, this is converted to $ACFH_{N2}$ using this formula:

Equation 4.1: ACFH formula

$$ACFH_{N_2} = \frac{SCFH_{Air}}{C} * \frac{T_A}{288.7K} * P_S P_A$$

Where:

$T_A = Operating\ Temperature\ (K)$

$C = Correction\ Factor\ (found\ from\ Matheson\ Gas)$

$P_S = Pressure\ at\ STP\ (1\ atm)$

$P_A = Operating\ Pressure\ (\sim 1\ atm)$

The correction factor used is found from Matheson Gas [46] in the form of:

Equation 4.2: Correction factor equation

$$SCFH_{Air} = SCFH_{N_2} * C$$

Or

Equation 4.3: Revised correction factor equation

$$SCFH_{N_2} = \frac{SCFH_{Air}}{C}$$

The operating pressures of the auger reactor are not constant and due to the maximum pressure of the reactor, must be less than 2 psig. However, since the reactor vents to the atmosphere, any fluctuations in pressure will remain small, well below 2 psig. This difference was considered negligible.

The minimum rotameter measurement is 6 $SCFH_{Air}$ for the maximum residence time. When C is set to 0.98 for N_2 and T_A is set to 773.15 K, the $ACFH_{N2}$ equals 16.4 ft^3/hr

The residence time for the auger section of the reactor was calculated in seconds as:

Equation 4.4: Vapor residence time

$$t = \frac{1}{ACFH_{N_2}(4/(\pi({r_o}^2 - {r_i}^2) * length * C_{baffling}))}$$

For the given flow conditions, the residence time was calculated to be 10.9 s.

It is important to note that this equation does not take into account gases produced in the reactor; introducing more gas into the flow will increase the flow, since the reactor is not pressurized. However, there is currently no accurate way of measuring how much gas is produced or what its properties are. While measuring the mass collected is possible, the density of the gas is not known.

These equations were used to calculate the gas residence times for 6 cfm, 10 cfm, and 20 cfm. The corresponding gas residence times were found to be 11 seconds, 6.5 seconds, and 3.2 seconds, respectively for an auger temperature of 500°C.

4.1.1.6. Gas flow rate study results

There was a slight increase in energy content in the LVBO, while the HVBO experienced no observable significant changes. However, the mass fraction of the oil recovered declined steadily with decreasing residence time, while the char collection rose correspondingly. In addition, buildups of char occurred in the transition pipe at the lower residence times. It was determined to set the gas flow rate at 6 cfm, or an for all future tests. Table 4.3 shows the results of the study, while Table 4.4 shows the variation in the residence time with the reactor temperature.

Table 4.3: Gas Residence Time Study Results

	Gas Residence Time		
Results	11 sec	6.5 sec	3.2 sec
LVBO Energy Content (kJ/kg)	7854	8351	8473
HVBO Energy Content (kJ/kg)	27322	27065	27573
Total Oil Yield (mass fraction)	0.37	0.32	0.30
Char Yield (mass fraction)	0.41	0.42	0.43

Table 4.4: Residence Time as a Function of Reactor Temperature

Reactor Temp.	Residence Time
400°C	12.5 sec
450°C	11.6 sec
500°C	11 sec
550°C	10.2 sec
600°C	9.6 sec

4.2. Main Experiment Data and Analysis

4.2.1. Two-factor repeatability analysis

In order to determine if the reactor could produce results that were repeatable regarding the oil properties, two runs were duplicated for analysis. Due to equipment malfunction, the first set of LVBO was not tested for the 450-20 and 600-20 runs. All comparisons were made with the HVBO.

Table 13 shows the collection results for the 450-20 and the 600-20 tests. EC denotes energy content, in kJ/kg; TAN denotes total acid number, in mg KOH/g oil; and KF denotes water content (as found through the Karl-Fisher method), in percent water.

Table 4.5: Two-run comparisons of 450-20 and 600-20 for repeatability analysis

Reactor	Condenser	Time of Testing (days after run)	LVBO EC	HVBO EC	LVBO TAN	HVBO TAN	LVBO KF	HVBO KF	HVBO Yield	LVBO Yield	Char	Total Oil
450°C	20°C	1	7761	28578	71.917	18.417	65.14	12.32				
450°C	20°C	1	7648	27131	74.5	21.02	63.25	12.29	133 g	315 g	718 g	448 g
450°C	20°C	1	7526	27692	80.724	21.043	59.19	13.06				
450°C	20°C	1	--	27526	--	10.809	--	12.64				
450°C	20°C	1	--	27436	--	13.307	--	10.54	144 g	284 g	825 g	428 g
450°C	20°C	1	--	28164	--	15.398	--	11.35				
600°C	20°C	1	8010	28347	83.475	16.753	61.67	12.32				
600°C	20°C	1	8032	28326	71.042	16.71	60.27	12.29	265 g	316 g	461 g	581 g
600°C	20°C	1	7910	28119	80.475	18.016	60.63	13.06				
600°C	20°C	1	--	28037	--	14.998	--	11.89				
600°C	20°C	1	--	28360	--	15.842	--	11.73	309 g	321 g	477 g	630 g
600°C	20°C	1	--	27315	--	17.081	--	11.41				

Analysis of Variance (ANOVA) tests, performed by Minitab, were used to determine if the means differed from each other. The first to be analyzed was the 450-20H oil. Since only one test was performed for viscosity for each run, it will not be used in the ANOVA analysis. Figure 4.2-Figure 4.3Figure 4.4 show the results of the ANOVA analysis.

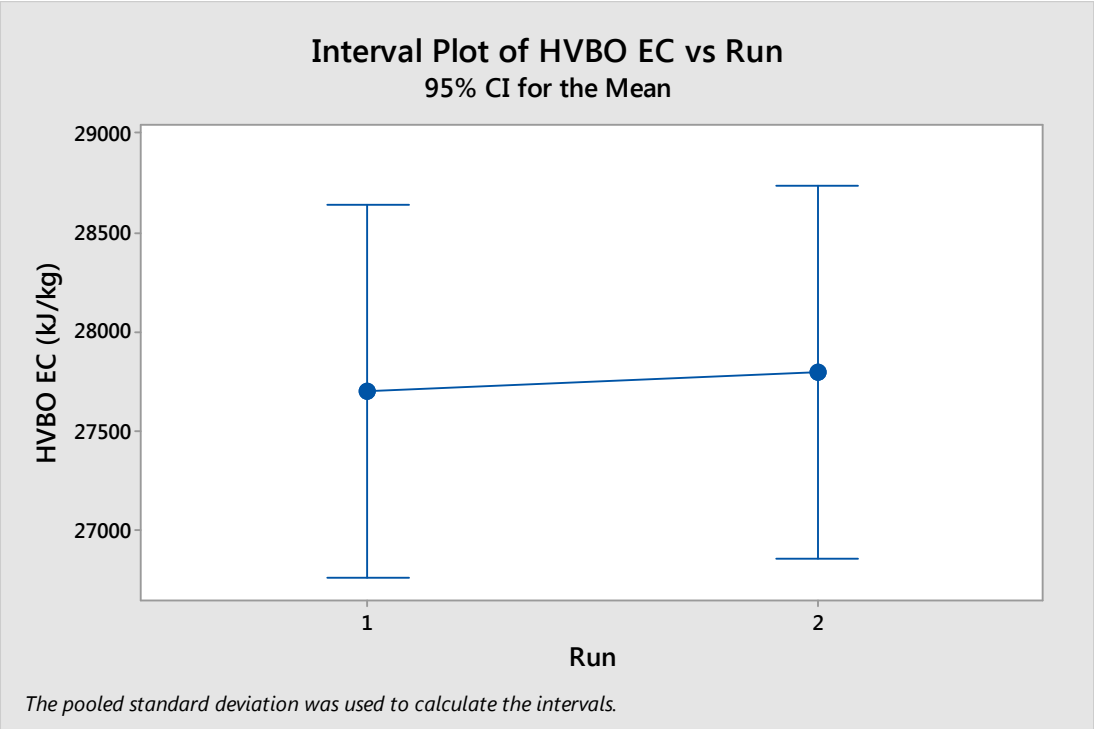

Figure 4.2: 450-20H Energy Content ANOVA Analysis

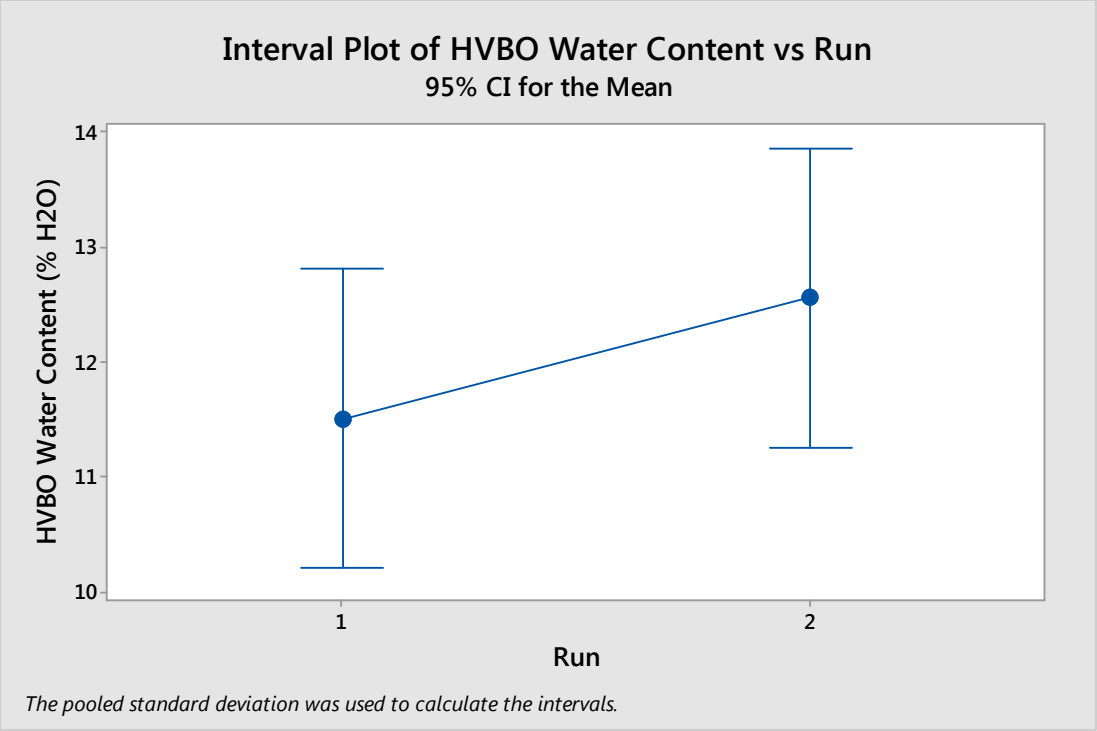

Figure 4.3: 450-20H Water Content ANOVA Analysis

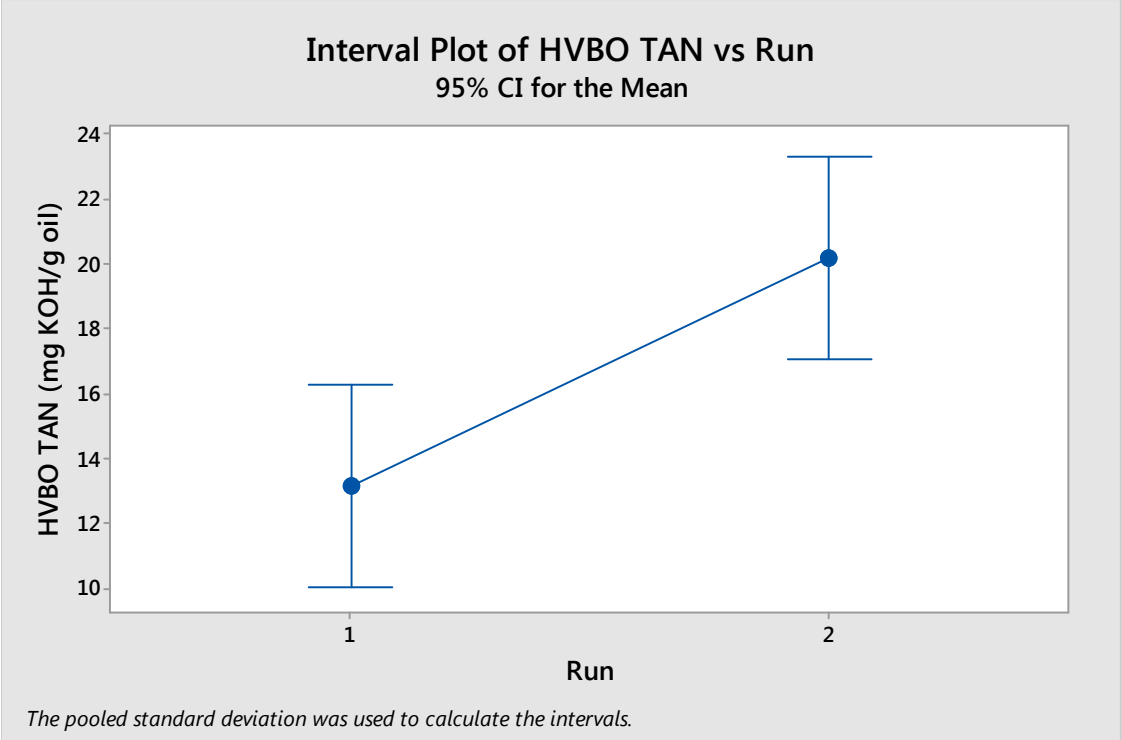

Figure 4.4: 450-20H TAN ANOVA Analysis

As can be seen from the interval plots in Figure 4.2 and Figure 4.3, there is no significant difference between the two runs of 450-20H in the energy content and the water content. There is a statistically significant difference between the two runs for the TAN. This could be attributed to a TAN calibration error on one of the tests. The 600-20H runs were analyzed for similar differences; the 600-20H ANOVA plots are shown in Figure 4.5-Figure 4.7.

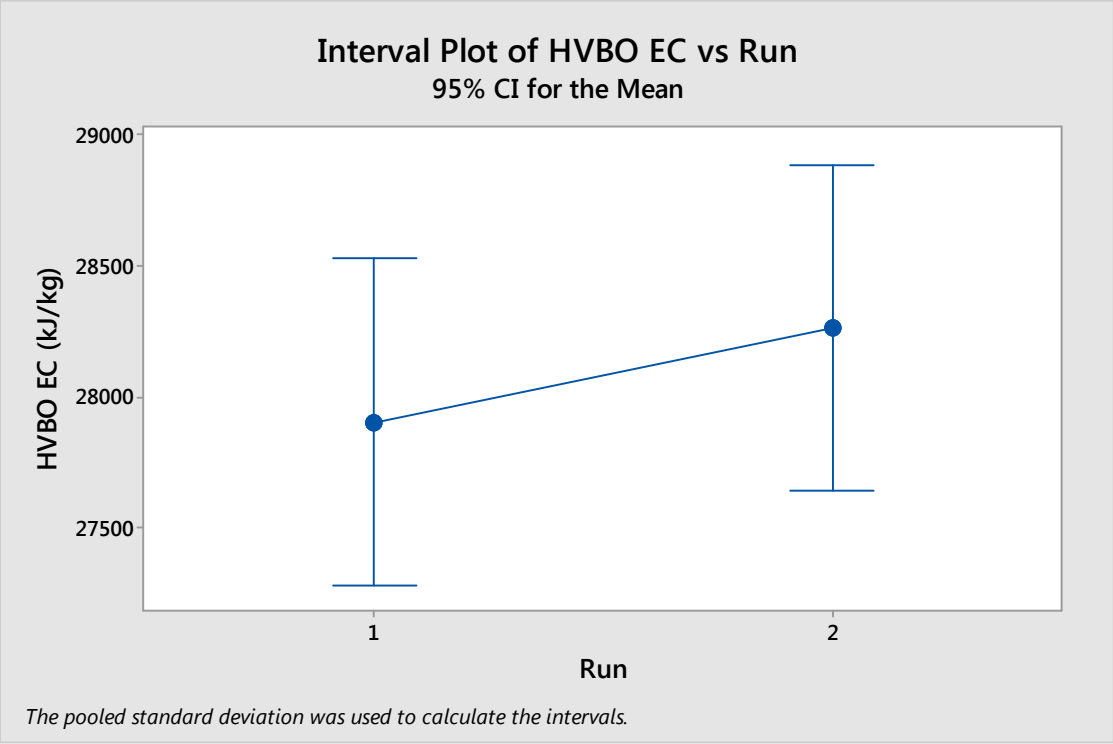

Figure 4.5: 600-20H Energy Content ANOVA Analysis

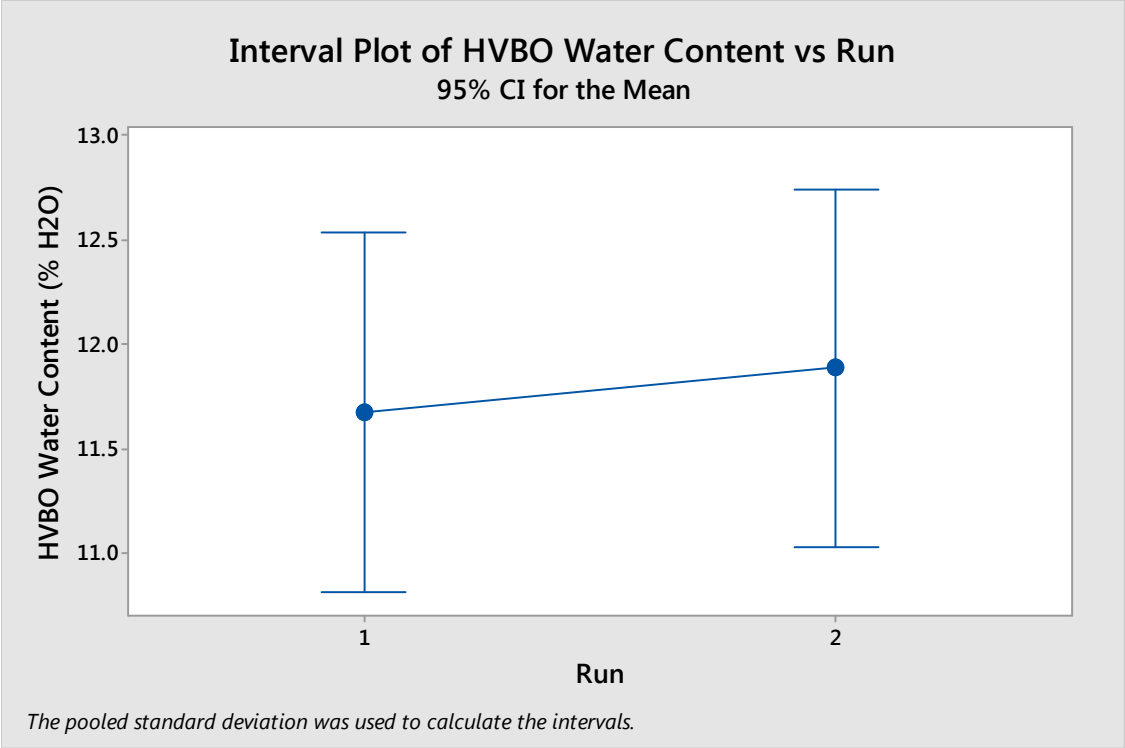

Figure 4.6: 600-20H Water Content ANOVA Analysis

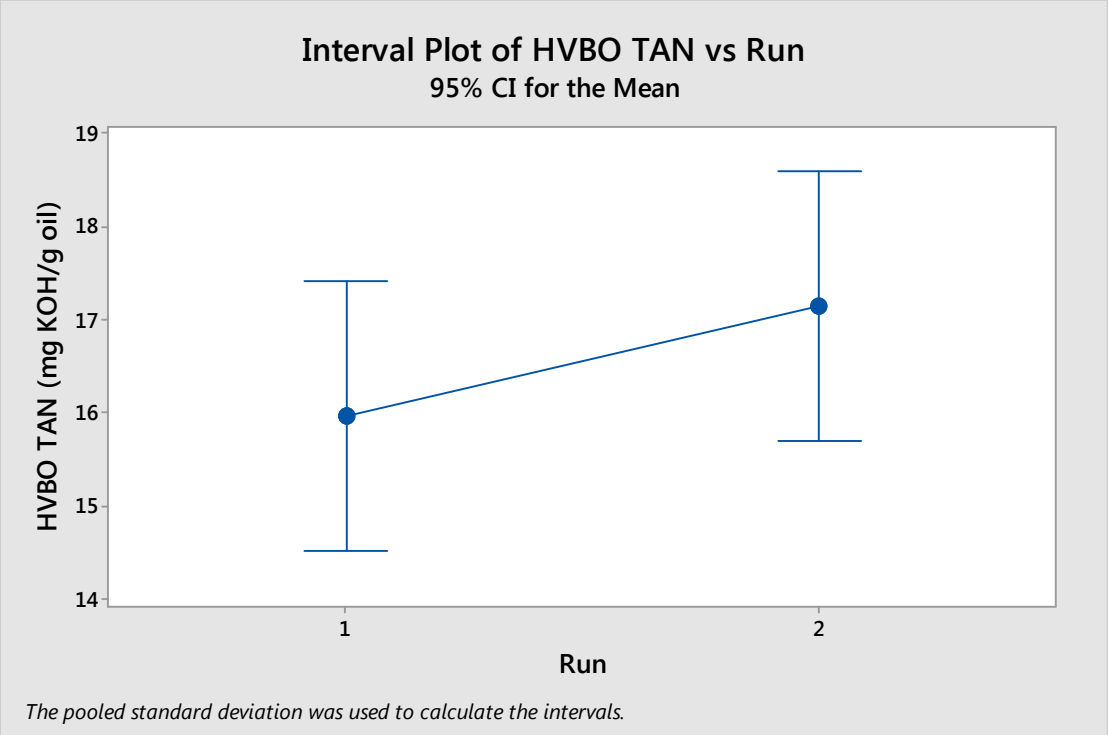

Figure 4.7: 600-20H TAN ANOVA Analysis

The TAN for the 600-20H tests do not show any significant differences between the means of runs 1 and 2; nor does the energy content. The KF has no statistically significant difference. TAN differences in the 450-20H runs were attributed to a calibration error that was found after the test was completed.

The viscosity was compared visually in Figure 4.8 by averaging the shear rates from 1-1000 rad/sec for the 25ºC, 50ºC, and 80ºC temperatures, then averaging the three temperature means to find a total average for the oil for ease of reporting. The viscosity was similar.

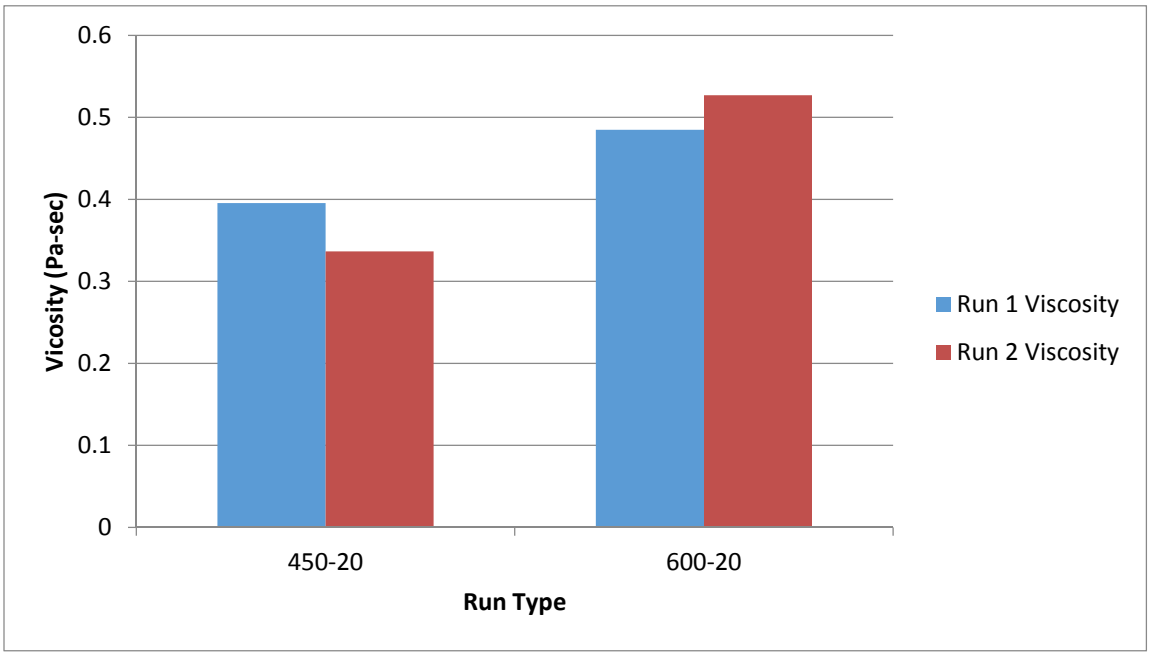

Figure 4.8: Viscosity Comparison for Repeatability

The yield was then analyzed for major fluctuations. Since the yield consistently showed the most variation out of all parameters recorded, it proved to be the most difficult to judge. Figure 4.9 shows the repeatability yield data.

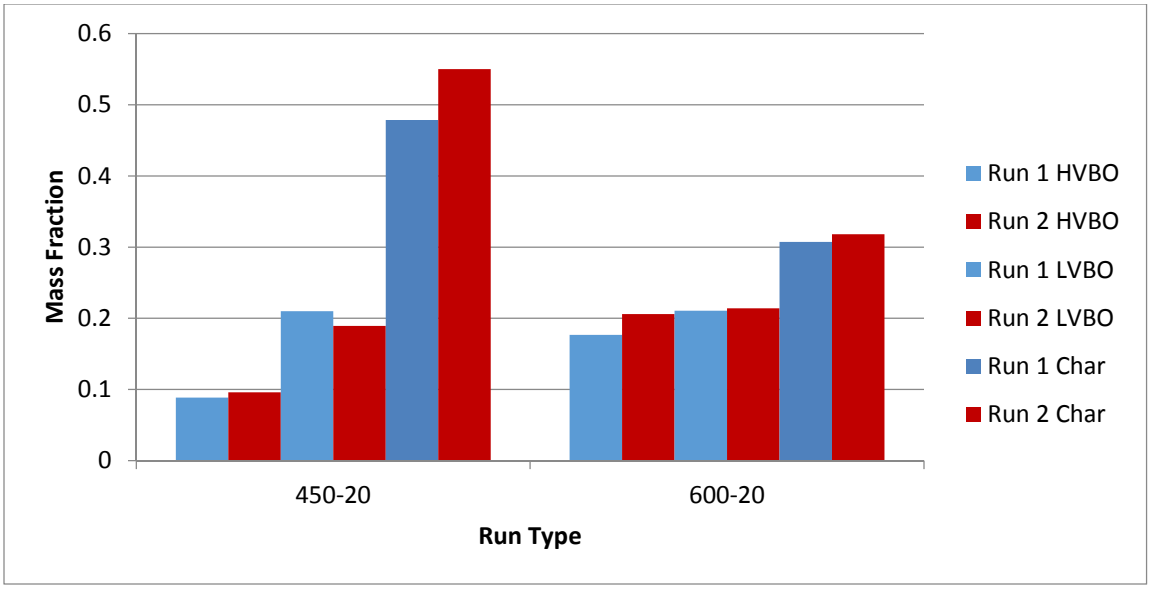

Figure 4.9: Yield Comparison for Repeatability

No major fluctuations were detected; however, the conclusion was drawn that the auger reactor could use some upgrades to reduce the yield fluctuations.

In summary, the auger reactor can produce repeatable results; deviations in the TAN and water contents should be scrutinized, as the root cause is unlikely to be caused by the reactor. Energy content is identical between runs. Viscosity proved to be similar, and the yield information is unlikely to be a reliable source regarding repeatability.

4.2.2. Yield Analysis

The 400-20 run was quickly removed from the analysis; the process was closer to torrefaction than pyrolysis, and the oil was difficult to test due to its high water content, high TAN, and difficulty in separating the LVBO from the HVBO. In addition, not enough HVBO was collected to perform the aging experiments due to an extremely poor yield. Figure 4.6 shows the results for the 400-20 oil. EC denotes energy content, in kJ/kg; TAN denotes total acid number, in mg KOH/g oil; and KF denotes water content (as found through the Karl-Fisher method), in percent water.

Table 4.6: 400-20 Results

Reactor	Condense	Time of test (days after run)	LVBO EC	HVBO EC	LVBO TAN	HVBO TAN	LVBO KF	HVBO KF	LVBO visc.	HVBO visc.	HVBO Yield	LVBO Yield	Char	Total Oil
400°C	20°C	1	--	25711	--	18.064	--	17.2	--	0.4868				
400°C	20°C	1	--	24446	--	90.469	--	17.87	--	0.4868	57 g	183 g	1021 g	240 g
400°C	20°C	1	--	25083	--	85.979	--	16.49	--	0.4868				

Due to the lack of repeatability, no standard deviations can be calculated. However, since the repeatability study showed that yield data could vary as much as 30% for one run, this presents a pretty broad window for checking the differences. The total mass recovery is shown in Table 4.7 and Figure 4.10.

Table 4.7: Mass Recovery Results

Collection	Yield (mass fraction)					
Species	Light Oil		Heavy Oil		Char	
Reactor Temp.	Condenser Temp.		Condenser Temp.		Condenser Temp.	
	20°C	**40°C**	**20°C**	**40°C**	**20°C**	**40°C**
400°C	0.12	--	0.04	--	0.68	--
450°C	0.21	0.19	0.09	0.13	0.48	0.48
500°C	0.19	0.22	0.11	0.20	0.47	0.35
550°C	0.21	0.19	0.12	0.18	0.31	0.42
600°C	0.21	0.20	0.18	0.20	0.31	0.31
500°C Cat	--	0.19	--	0.12	--	0.51

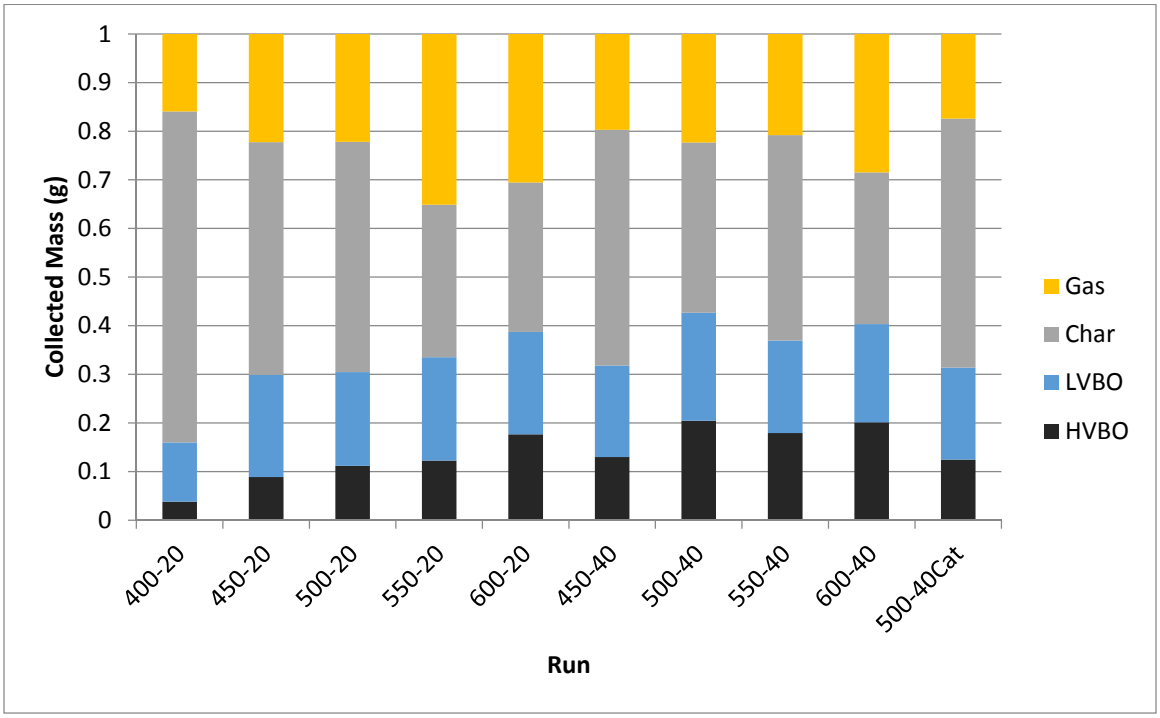

Figure 4.10: Total Mass Recovery Results, Mass Fraction

There is a general trend in the HVBO collection in the 20°C condenser temperature; as the reactor temperature rises, so does the mass of HVBO collected. For the 40°C condenser temperature, the higher temperatures appear to all have roughly the same yield. It's worth noting that the 500-40Cat catalyst run had much less yield than its 500-40 counterpart.

The LVBO yield data doesn't show any significant trends—all points, except for the 400-20 run, fall between 250g to 350g of LVBO recovery. The 400-20 run is significantly lower, due to the fact that the lower auger temperatures were not conducive to fast pyrolysis and not much reaction taking place.

The char yield for the collection for the 20°C condenser temperature follows a general trend; as the reactor temperature rises, the mass of char collected falls. The general trend follows for the 40°C condenser temperature, with a fluctuation at the 550-40 run; this could be explained by char from the 500-40 run becoming lodged in the auger unit somewhere and falling out during the 550-40 run. If true, the 500-40 run would be a bit more and the 550-40 run being a bit less, as far as char collection goes. However, since the HVBO 550-40 was so much lower than the 500-40, and since the lower HVBO yield came with a corresponding increase in char collection, it is more likely that the auger lost temperature at some point during the run and did not fully pyrolyze parts of the biomass. Programming on the reactor has since been updated to provide better temperature control.

As can be seen in Figure 4.10, the collected bio-oil, combined HVBO and LVBO, never reaches 50%. However, the collection is in two different types of oil. At least 15% of the biomass input is lost to the filter/atmosphere vent.

This is a marked change from what was reported in the literature review. The physical behavior of this particular reactor is likely the root cause of the low yields here. As discovered during the solids residence time test, the longer the solids are allowed to remain in the reactor, the more oil is collected. However, the auger jams if the solids feed rate is set to feed too slowly. This could be due to poor insulation in areas of the reactor leading to uneven thermal expansion on the auger. The auger itself could also be damaged in some way; this would also need to be investigated. Should neither of these issues be the root cause, there are still two other ways to combat this problem.

The first is to replace the motor with something that has greater torque at lower speeds. This would enable the auger to keep turning in order to power through the higher resistance. If the auger is undamaged and thermal expansion isn't a concern, the higher resistances are likely due to char sticking to the reactor walls. The second method would be to extend the reactor itself, and allow the current speed to carry the biomass through a longer heated section to extend the time of pyrolysis. It is possible that a batch method could be used as well—feeding the biomass into the reactor and then turning the auger off, letting the biomass sit in the reactor—but that could cause the char to stick to the walls in a way that would render it impossible for the auger to remove it later. Further study is warranted here.

4.2.3. Energy content as a function of reactor temperature, condenser temperature, and aging

Energy content was measured with the bomb calorimeter. Instrument calibration was checked once per week. The bio-oil was measured in sample sizes of 0.2 grams. The bio-oil being tested was mixed with a mineral oil to aid combustion, with 0.54 grams

being added to the LVBO and 0.44 grams being added to the HVBO. The mineral oil's energy content was then accounted for during the test to find the bio-oil energy content. Each test was run three times to produce a mean and deviation for the day's tests and to give it the necessary data for an ANOVA and Fisher test.

4.2.3.1. LVBO energy content analysis and trends

The LVBO energy content was similar. The 20°C condenser temperature had a lower energy content than the 40°C condenser setting, possibly because slightly more water was being caught and collected with the oil. Energy content for the LVBO is listed below in Table 4.8, and the interval plots for the reactor and condenser temperatures in Figure 4.11-Figure 4.13.

Table 4.8: LVBO Energy Content

LVBO	Energy Content (kJ/kg)									
Day	1		7		14		28		84	
Reactor Temp.	Condenser Temp.		Condenser Temp.		Condenser Temp.		Condenser Temp.		Condenser Temp.	
	20°C	**40°C**	**20°C**	**40°C**	**20°C**	**40°C**	**20°C**	**40°C**	**20°C**	**40°C**
400°C	--	--	--	--	--	--	--	--	--	--
450°C	7645	8036	7600	7952	7265	7915	7282	7994	7537	8010
500°C	7513	8404	7771	8262	7784	8142	7899	8245	7921	8281
550°C	7881	8308	7922	8397	7823	8556	7901	8510	7814	8600
600°C	7984	8625	7922	8377	7988	8090	7381	8212	7679	8527
500°C Cat	--	8064	--	7785	--	7790	--	7660	--	8013

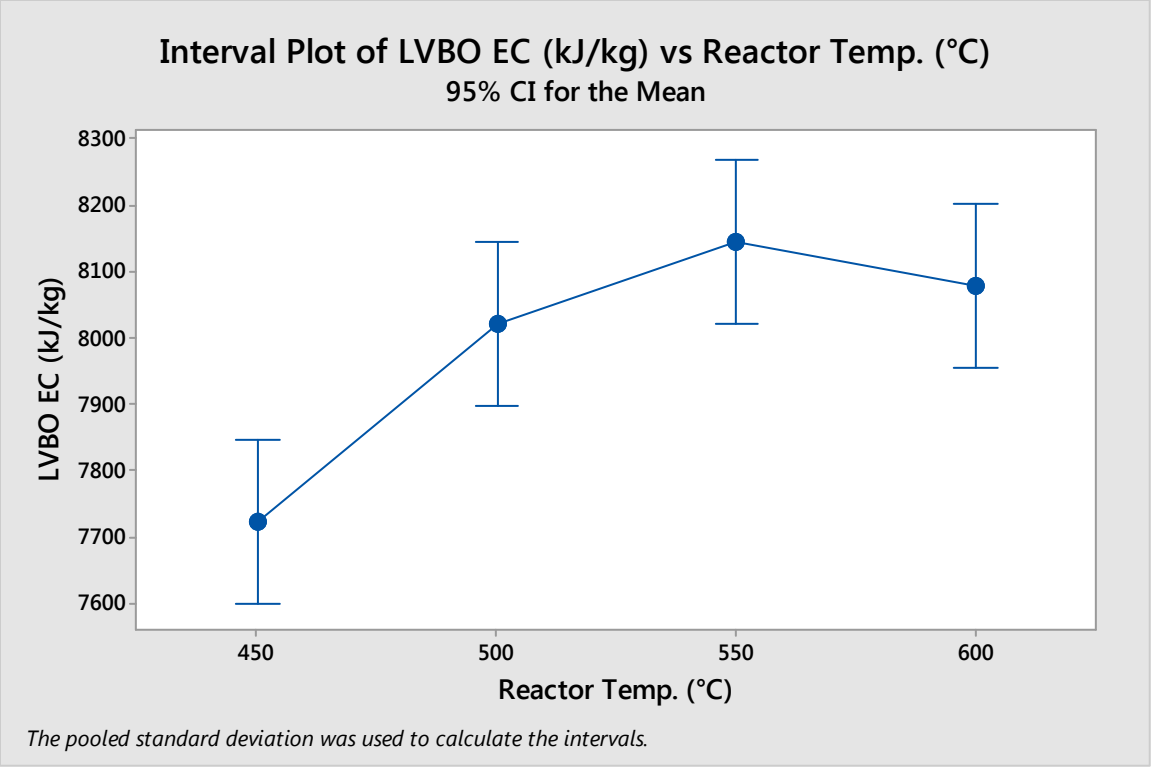

Figure 4.11: Interval plot for LVBO Energy Content vs Reactor Temperature

Figure 4.11 shows a significant difference between the 450°C condenser temperature and the 500°C, 550°C, and 600°C condenser temperatures. The Fisher test confirmed this; there was no statistically significant difference between the three highest temperatures, but a significant difference between those three and the 450°C reactor temperature. The trend, then, would seem to be lower reactor temperatures reduce the energy content of the LVBO, but a constant energy content is reached at 500°C and above. The difference is only a matter of roughly 300 kJ/kg between the 450°C and the other reactor temperatures; standard deviation for bomb calorimeter measurements is 200 kJ/kg.

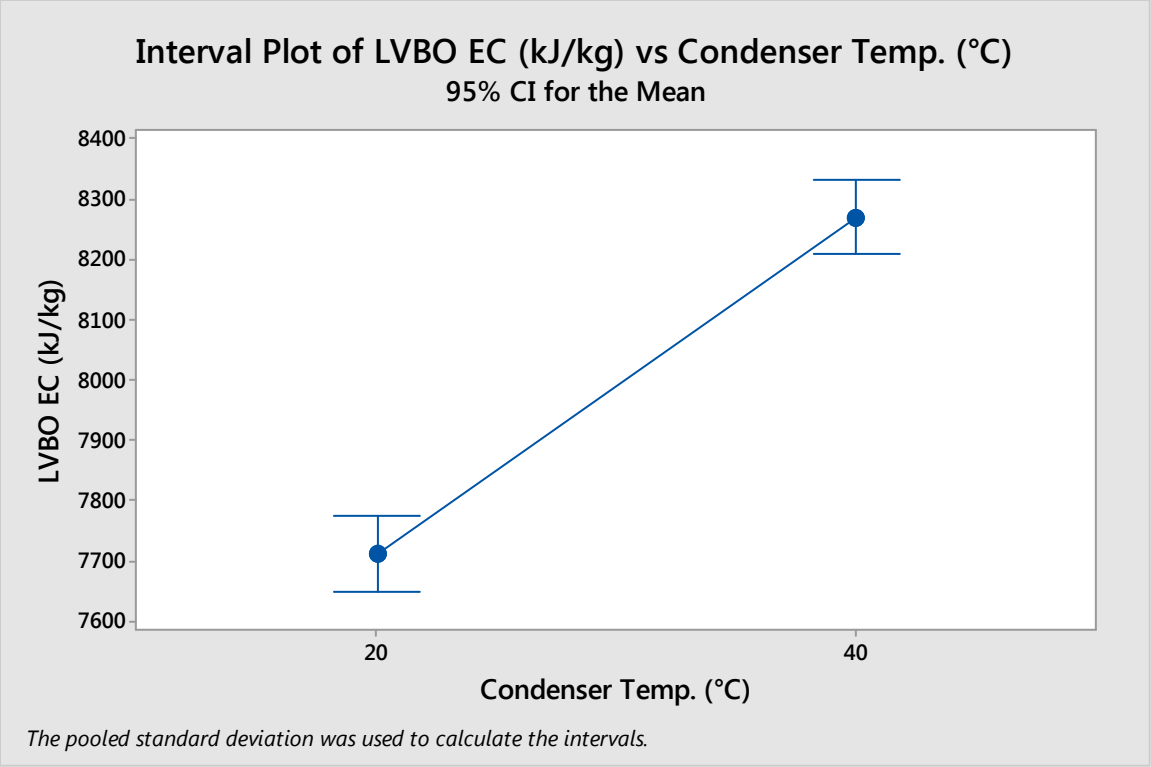

Figure 4.12: Interval plot for LVBO Energy Content vs Condenser Temperature

As can be seen in Figure 4.12 and in Table 4.8, the condenser temperature plays a large role in the energy content of the LVBO. There is nearly a 1.0 MJ/kg energy content difference between the lower and higher condenser temperatures; this could be attributed to a greater percentage of water being condensed at the lower temperatures. This also affects the water content. Higher condenser temperatures lead to greater energy content.

There was no significant aging effect for the energy content of the LVBO. The interval plot of LVBO energy content verses time is shown in Figure 4.13.

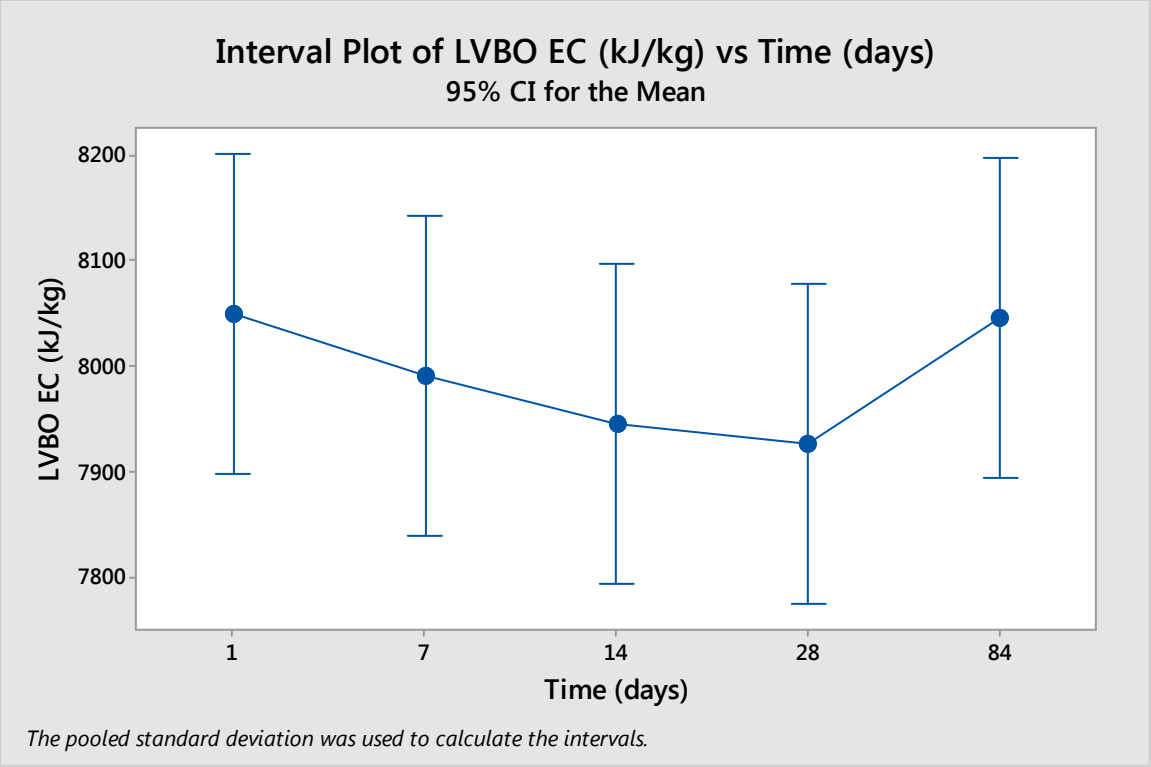

Figure 4.13: Interval plot for LVBO Energy Content vs Time

4.2.3.2. HVBO energy content analysis and trends

The HVBO energy content is considerably higher than the LVBO energy content; where LVBO ranges from 7 to 8 MJ/kg, HVBO ranges between 27-30 MJ/kg. HVBO shows similar trends as the LVBO, where condenser temperature has a large effect and reactor temperature has a slight effect between 450°C and the higher reactor temperatures. This can be seen in Table 4.9, but the ANOVA and Fisher tests were performed to analyze the exact differences and trends. The interval plots are below in Figure 4.14-Figure 4.16.

Table 4.9: HVBO Energy Content

HVBO	Energy Content (kJ/kg)									
Day	1		7		14		28		84	
Reactor Temp.	Condenser Temp.		Condenser Temp.		Condenser Temp.		Condenser Temp.		Condenser Temp.	
	20°C	**40°C**	**20°C**	**40°C**	**20°C**	**40°C**	**20°C**	**40°C**	**20°C**	**40°C**
400°C	25080	--	--	--	--	--	--	--	--	--
450°C	27800	28216	30037	29317	30057	28838	29253	29272	30033	29558
500°C	27328	27155	27974	26886	28657	27281	28978	27944	27526	28259
550°C	27558	27375	27979	27321	29015	27786	29437	27791	28965	28323
600°C	28264	26786	28789	27515	29332	27176	29364	27317	27109	28630
500°C Cat	--	27651	--	27584	--	28607	--	28701	--	28777

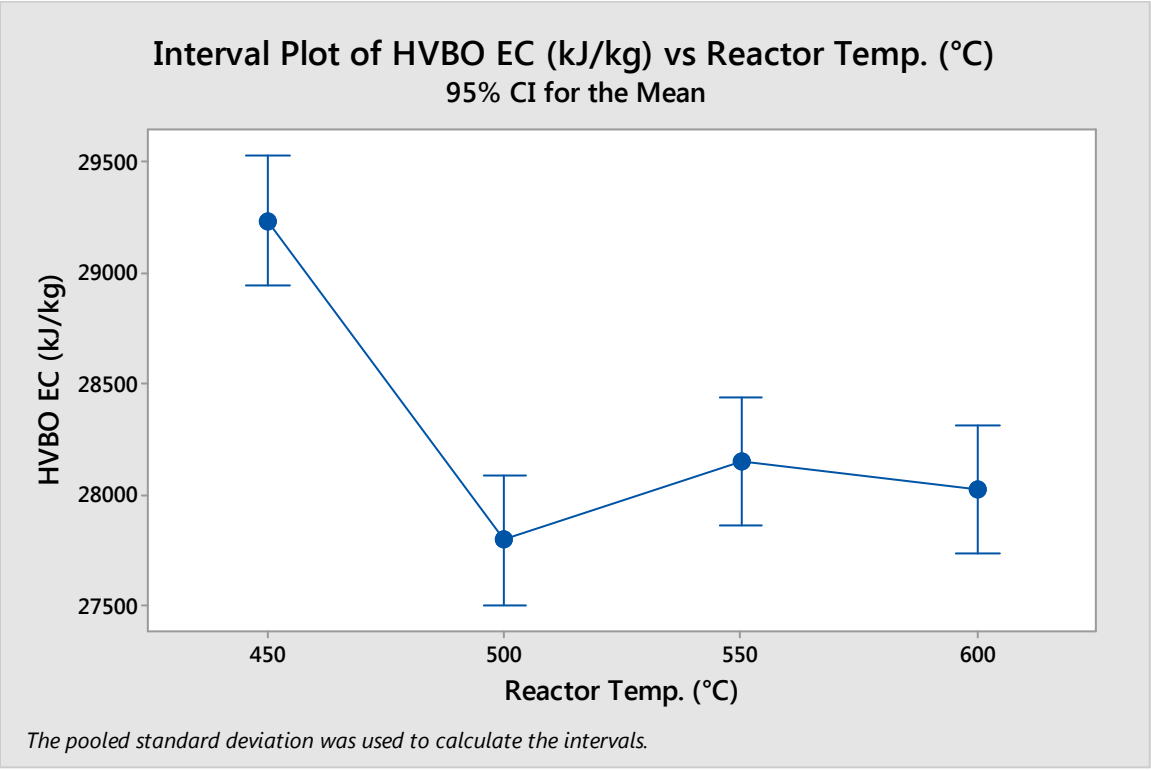

Figure 4.14: Interval plot for HVBO Energy Content vs Reactor Temperature

HVBO energy content drops dramatically from an average of 29.2 MJ/kg to an average around 28 MJ/kg from the 450°C reactor temperature to the 500°C-600°C reactor temperatures. This is the reverse of the LVBO trend seen before, where the energy content increased. However, the difference here is more drastic (1.2 MJ/kg difference as opposed to 0.3 MJ/kg). The same type of "leveling out" or cap on the temperature is present, as the Fisher test confirms no significant differences between 500°C, 550°C, and 600°C conditions.

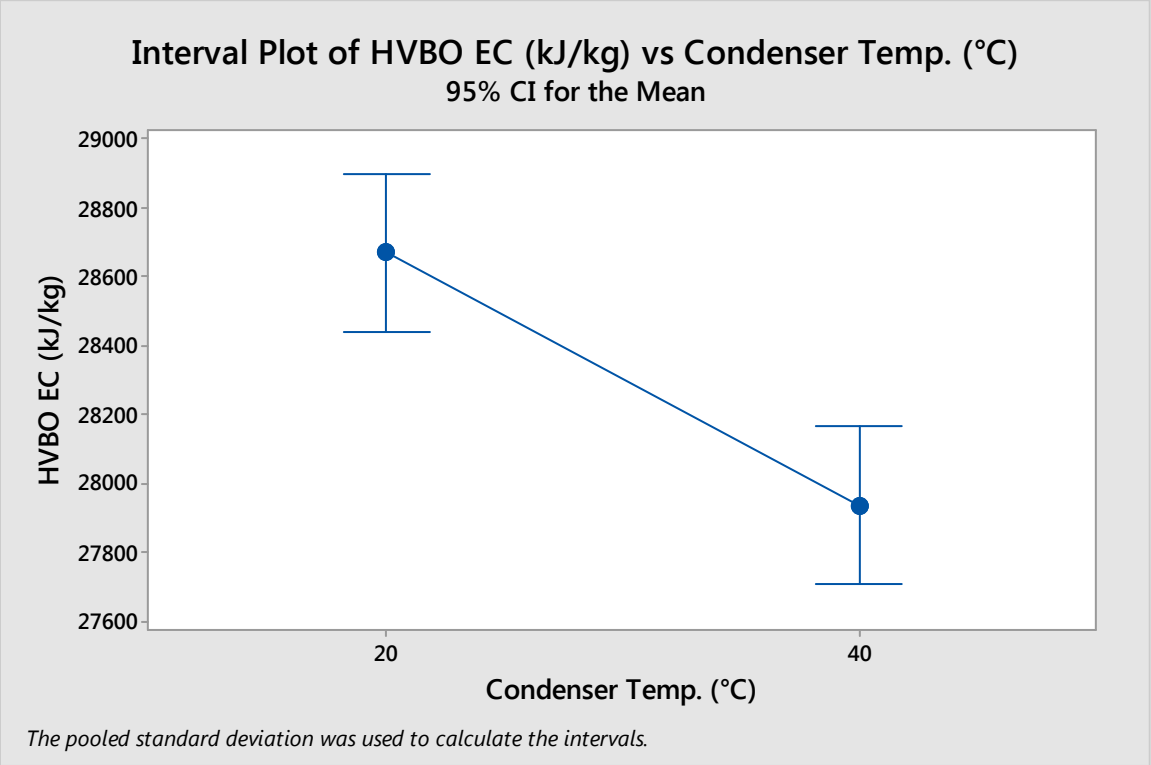

Figure 4.15: Interval plot for HVBO Energy Content vs Condenser Temperature

Between the lower and higher condenser temperatures, the HVBO energy content differs by 0.8 MJ/kg; this is a large difference, but not quite as large of an effect as the reactor had on the energy content of the HVBO. Once again, the trend is the opposite of the LVBO condenser trend. Lower condenser temperatures here correlate to higher

energy contents for HVBO. This could be because more volatiles are condensed at the lower condenser temperatures.

There was a mild increase in energy content between the first test and the 7-day test, but no statistically significant difference in the energy content between the 7-, 14-, 28-, and 84-day tests. The interval plot is below in Figure 4.16.

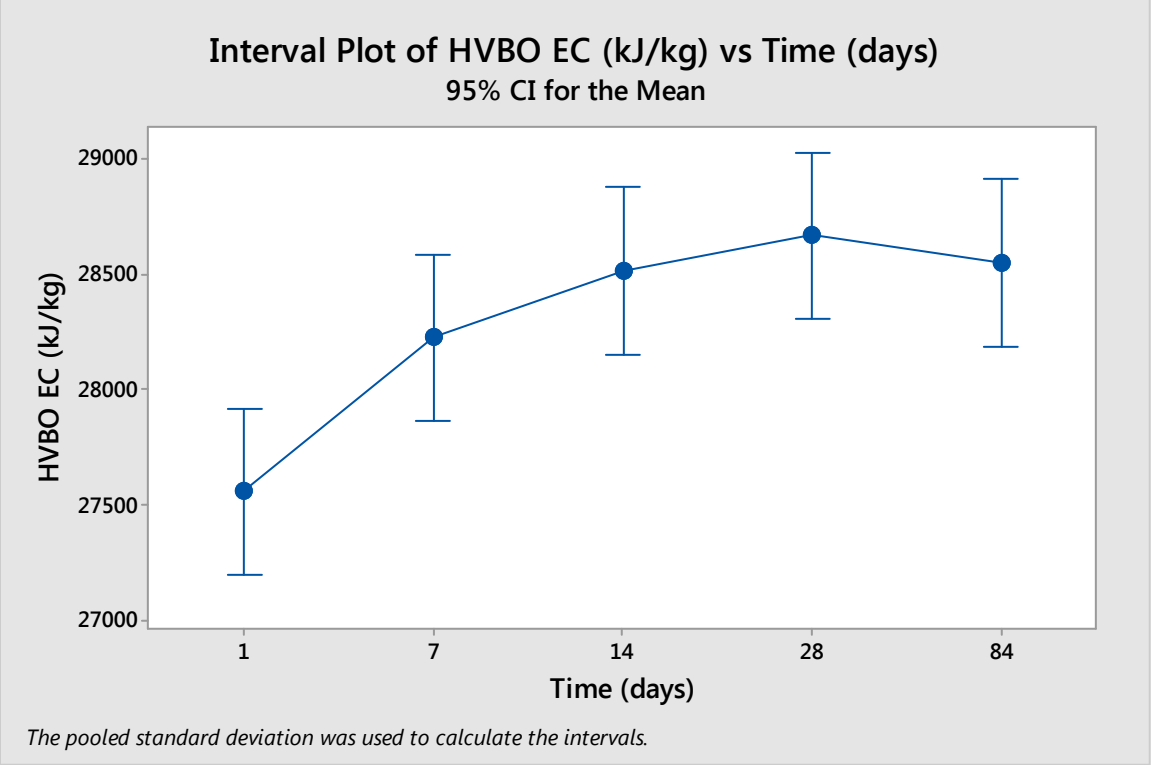

Figure 4.16: Interval plot for HVBO Energy Content vs Time

4.2.4. Water content as a function of reactor temperature, condenser temperature, and aging

Water content was found using the Karl-Fischer method of titration. The method was calibrated once per week, as the titer strength changed over time. Some deviations were noted due to improper calibration for a few measurements. One to two drops of each type of bio-oil was measured for analysis; roughly 0.006g of LVBO and 0.01g of HVBO.

Each test was performed three times to produce a mean and deviation for the day's test and to give it the necessary data for an ANOVA and Fisher test.

4.2.4.1. LVBO water content analysis and trends

It is difficult to see any immediate trends in the water content in Table 4.10. There is a point at 500-20 that was the result of an improper calibration; it was removed from the statistical tests. There does, however, appear to be a difference in water content due to changes in condenser temperatures. Figure 4.17-Figure 4.19 show the interval plots for the tests.

Table 4.10: LVBO Water Content

LVBO	Water Content (% H2O)									
Day	1		7		14		28		84	
Reactor Temp.	Condenser Temp.		Condenser Temp.		Condenser Temp.		Condenser Temp.		Condenser Temp.	
	20°C	**40°C**	**20°C**	**40°C**	**20°C**	**40°C**	**20°C**	**40°C**	**20°C**	**40°C**
400°C	--	--	--	--	--	--	--	--	--	--
450°C	62.53	61.32	65.04	61.62	61.36	66.17	65.94	64.05	63.41	63.00
500°C	60.04	60.09	94.34	60.55	60.95	58.58	66.38	60.62	61.34	62.48
550°C	60.02	59.02	60.11	58.10	67.57	58.95	61.47	61.18	60.77	63.02
600°C	60.86	56.92	61.06	55.88	59.89	60.40	61.42	66.34	60.62	59.43
500°C Cat	--	61.98	--	61.36	--	57.38	--	64.02	--	62.12

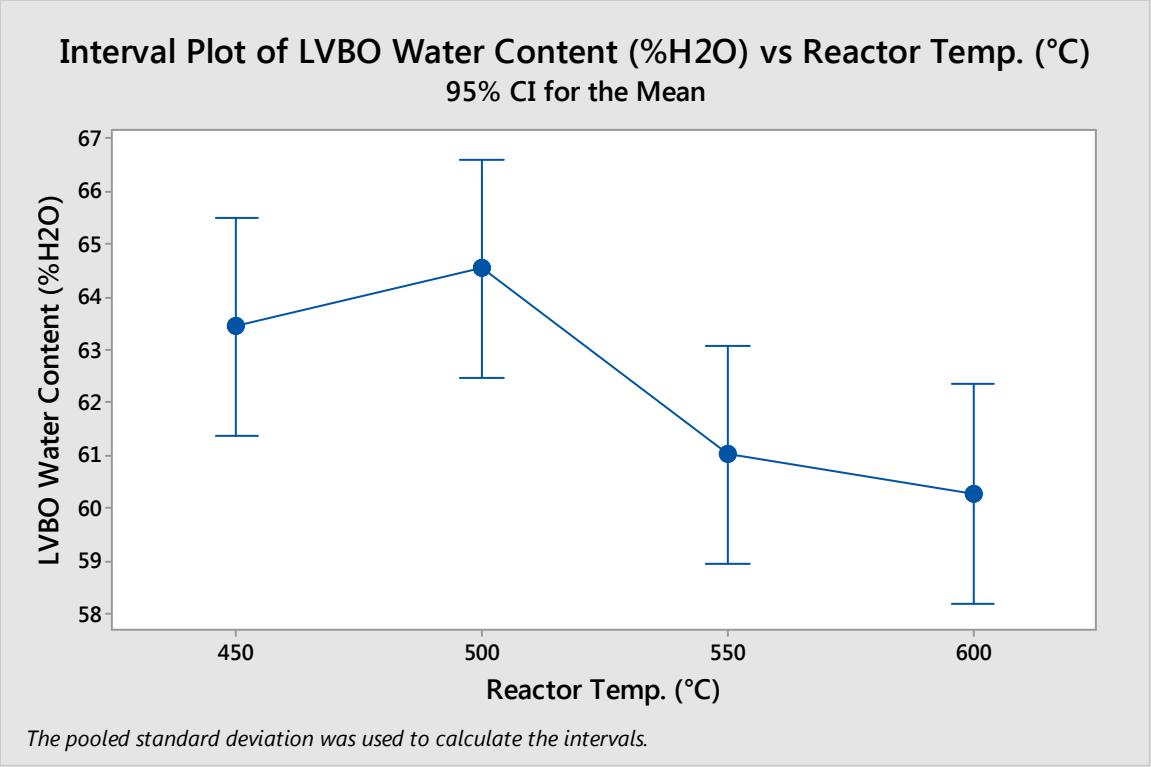

Figure 4.17: Interval plot for LVBO Water Content vs Reactor Temperature

The Fisher test states that there is no statistically significant difference between the 450°C and 500°C temperatures, nor is there one between the 550°C and 600°C temperatures and the 500°C and 550°C temperatures. A significant difference exists between the 450°C and 600°C conditions, however, suggesting a gradual decline in water content with an increase in reactor temperature.

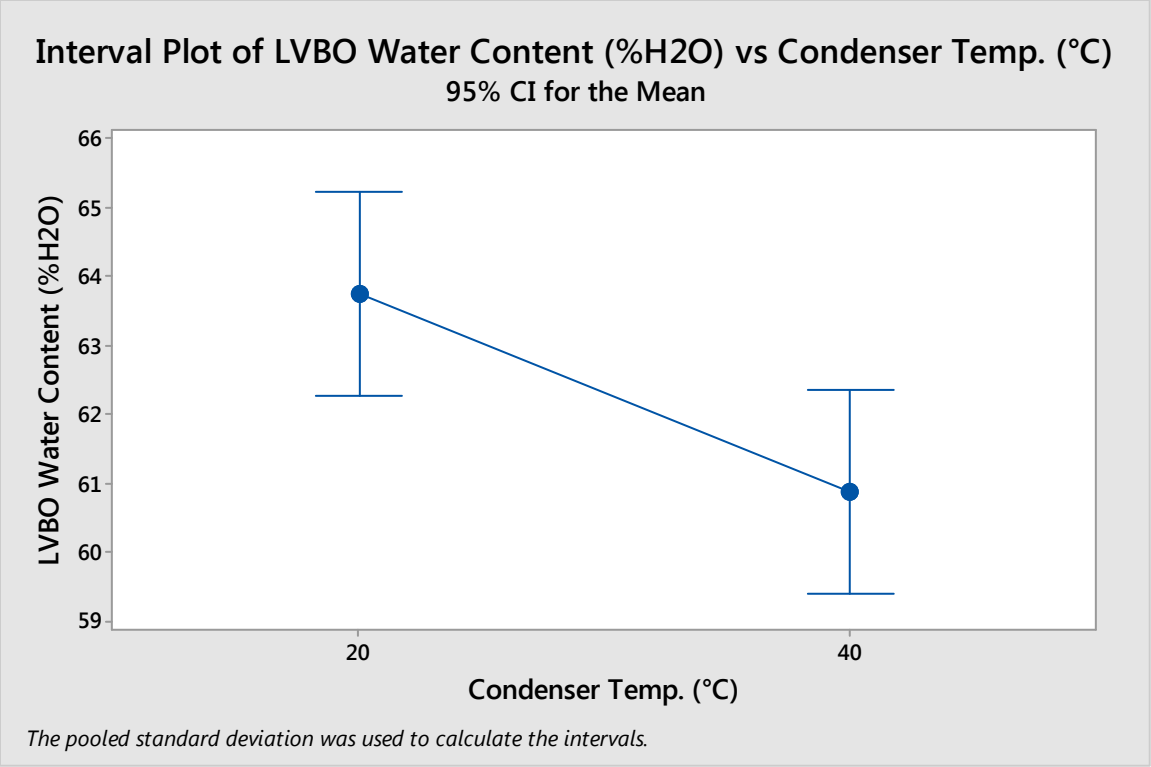

Figure 4.18: Interval plot for LVBO Water Content vs Condenser Temperature

The water content decreases markedly with increasing condenser temperature. The warmer the condenser is, the less water will be condensed out of the vapor stream as it is pushed through the condenser train by the nitrogen stream. This corresponds to the lower energy contents seen in the LVBO energy content analysis—the more water in the sample, the lower the total energy content will read, as water will not contribute to the overall energy output.

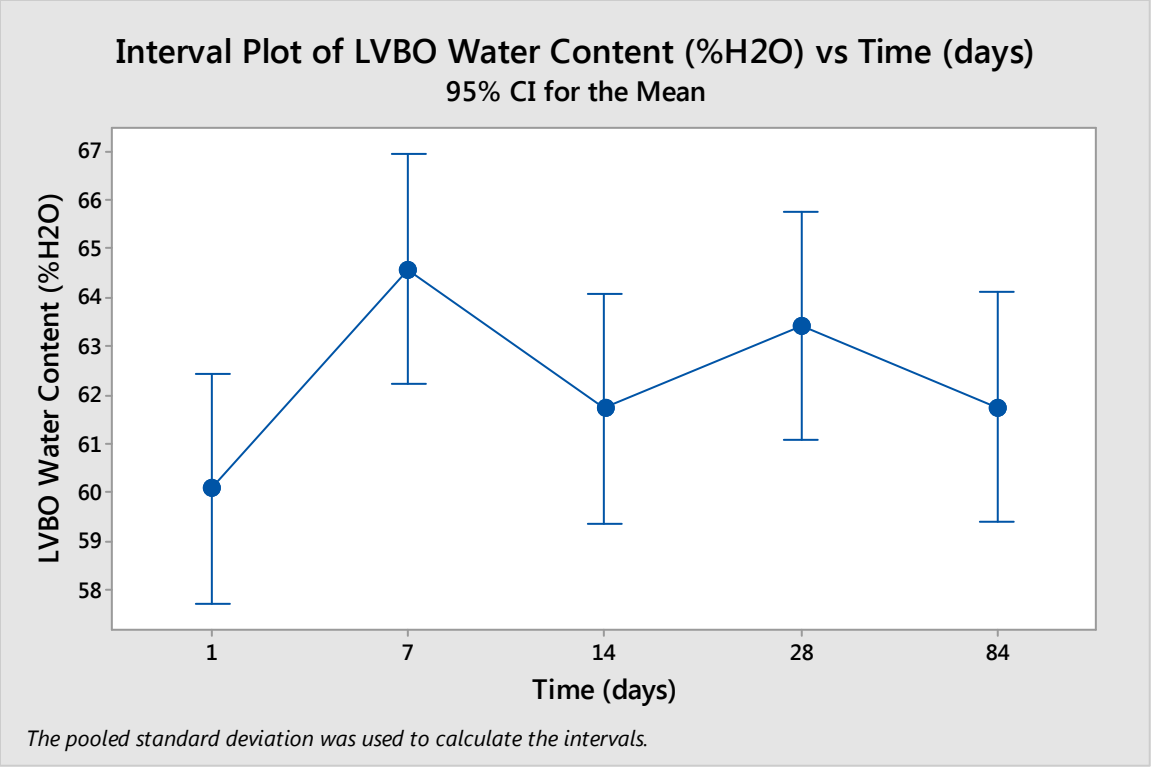

Figure 4.19: Interval plot for LVBO Water Content vs Time

There is no statistically significant difference in the water content as the LVBO ages.

4.2.4.2. HVBO water content analysis and trends

HVBO has a massively lower water content than the LVBO, as seen in Table 4.11. Once again, it would appear that this is similar to the LVBO analysis, with the lower water content corresponding to the lower reactor temperatures. This could explain the lower energy contents at the higher reactor temperatures seen in the energy content analysis of HVBO. The interval plots are shown in Figure 4.20-Figure 4.22.

Table 4.11: HVBO Water Content

HVBO	Water Content (% H2O)									
Day	1		7		14		28		84	
Reactor Temp.	Condenser Temp. 20°C	Condenser Temp. 40°C	Condenser Temp. 20°C	Condenser Temp. 40°C	Condenser Temp. 20°C	Condenser Temp. 40°C	Condenser Temp. 20°C	Condenser Temp. 40°C	Condenser Temp. 20°C	Condenser Temp. 40°C
400°C	17.19	--	--	--	--	--	--	--	--	--
450°C	12.56	11.97	8.41	10.92	8.01	9.36	14.48	9.47	7.95	9.38
500°C	13.07	12.24	14.86	12.52	10.29	13.00	9.06	11.54	11.32	12.22
550°C	13.92	12.67	12.62	12.11	9.55	12.48	8.78	11.58	8.77	12.59
600°C	12.56	14.53	9.54	12.14	11.56	16.47	8.47	13.11	13.87	11.24
500°C Cat	--	12.48	--	12.06	--	12.05	--	10.77	--	12.31

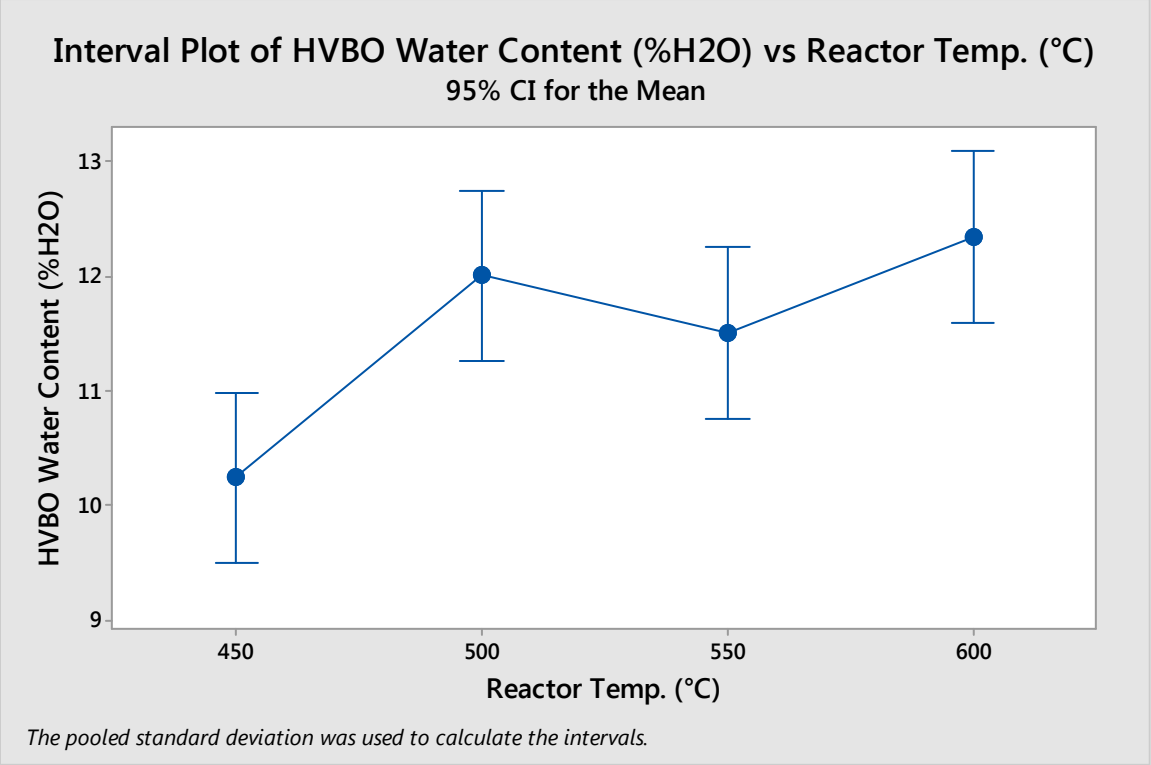

Figure 4.20: Interval plot for HVBO Water Content vs Reactor Temperature

Also seen in Figure 4.14 from the energy content analysis, the last three reactor temperatures are identical as shown by the Fisher test in Figure 4.20. This also corresponds to the lower energy contents seen in that particular analysis.

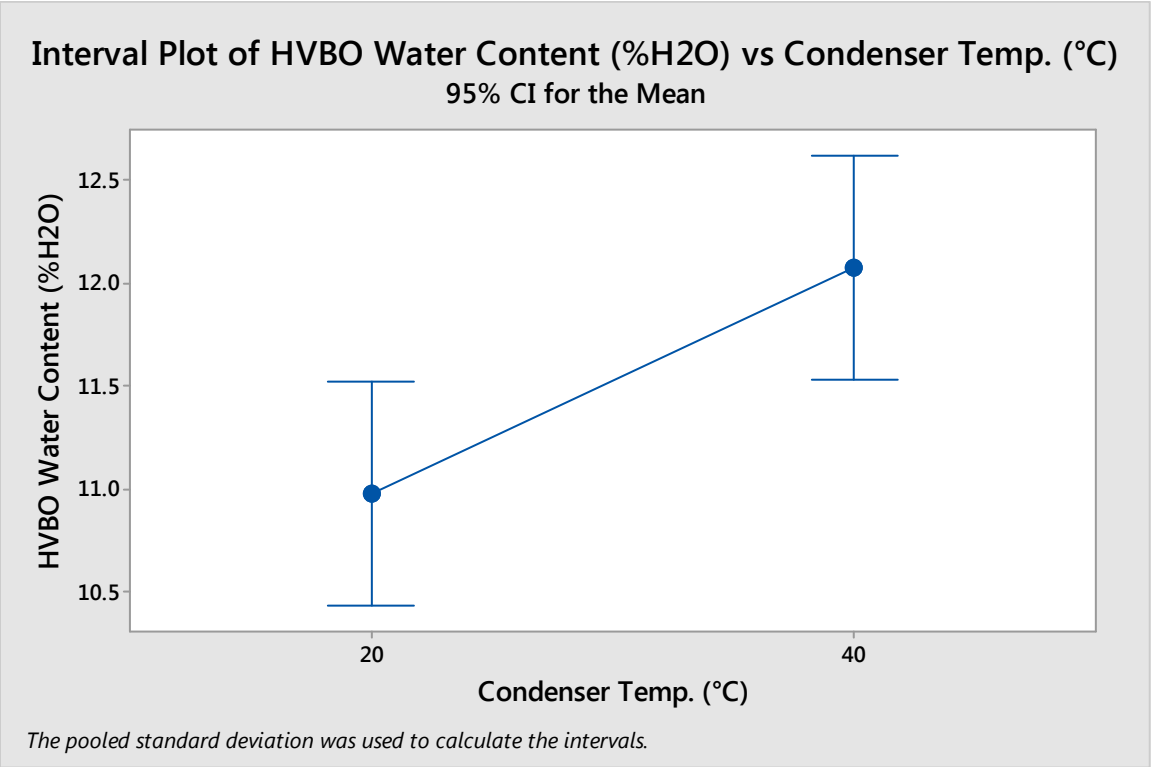

Figure 4.21: Interval plot for HVBO Water Content vs Condenser Temperature

The lower water contents in Figure 4.21 again match up to the energy contents in the previous analysis seen in Figure 4.15. The lower temperatures correspond to a lower water content. When compared with Figure 4.12, Figure 4.18, and Figure 4.15, it would appear that the lower temperatures condense more of a hydrophilic compound that binds to the water produced and condenses into the LVBO collection. This would explain the higher water content in the LVBO and the lower water content in the HVBO at the 20°C condenser temperature.

The changes associated with aging observed in the 7-, 14-, 28-, and 84-day tests is not statistically significant. However, the initial 1-day test is different from the others. This could be explained by some water evaporating during storage. Once the excess water evaporated, the rest of the water would remain trapped in the HVBO and create a constant water content for the rest of the tests. Figure 4.22 shows the interval plot for the aging of the water content.

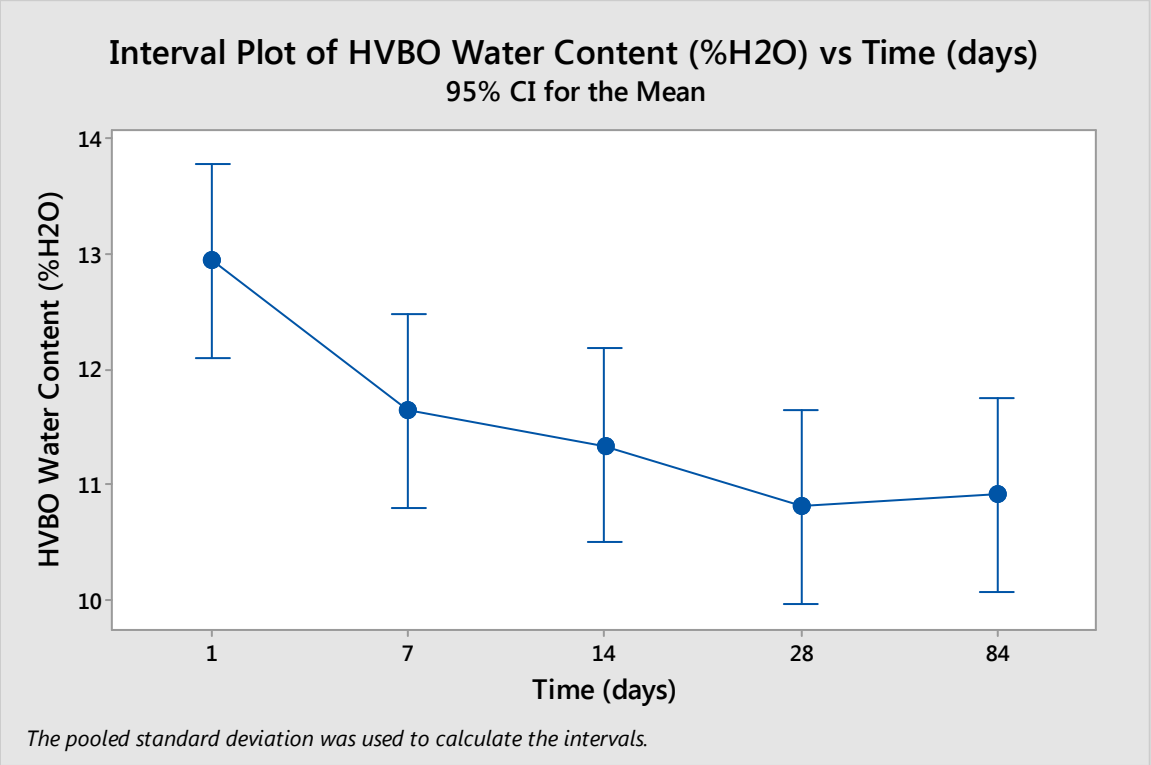

Figure 4.22: Interval plot for HVBO Water Content vs Time

4.2.5. Total acid number as a function of reactor temperature, condenser temperature, and aging

TAN was found using a titration method. The method worked as a standard titration, using an electrode to measure voltage differences across the prepared bio-oil

solution while adding titer until the solution was neutralized. The method was calibrated once per week, as the titer strength changed on a time basis. Some deviations were noted due to improper calibration for a few measurements. Two drops of LVBO were used for its analysis, while about eight drops were used for the HVBO analysis (0.01 g of LVBO and 0.12 g HVBO). Each test was run three times to produce a mean and deviation for the day's test and to give it the necessary data for an ANOVA and Fisher test.

4.2.5.1. LVBO TAN analysis

The TANs for the LVBO tended to be high, as seen in Table 4.12. Higher values, at first glance, seem to belong to the higher condenser temperatures, while no distinguishable pattern can be easily seen for reactor temperature or aging. However, there was some difficulty in measuring the properties. Several different procedures were used to calculate the TAN; the first procedure used was shown to have overshoot problems, where the TAN was shown to be higher than it was. Other procedures had wildly varying TANs or calibration issues, resulting in severe difficulty measuring the TAN. The standard deviation for the LVBO tests was found to be 12.0 mg KOH/g oil, suggesting large amounts of noise in the data.

ANOVA and Fisher analyses were completed in an attempt to shed some light on the error, as well as quantifying parameter differences. Figure 4.23-Figure 4.25 show the interval plots.

Table 4.12: LVBO TAN

LVBO	TAN (mg KOH/g oil)									
Day	1		7		14		28		84	
Reactor Temp.	Condenser Temp. 20°C	40°C	Condenser Temp. 20°C	40°C	Condenser Temp. 20°C	40°C	Condenser Temp. 20°C	40°C	Condenser Temp. 20°C	40°C
400°C	--	--	--	--	--	--	--	--	--	--
450°C	75.71	72.41	81.93	73.60	81.98	79.49	82.04	85.47	89.01	79.95
500°C	107.81	59.40	94.34	106.42	89.14	93.22	76.42	90.64	77.32	79.13
550°C	73.40	62.00	70.77	106.61	74.13	102.46	81.37	89.83	80.88	87.63
600°C	78.33	98.26	81.69	87.04	69.88	92.20	81.78	89.17	76.63	92.43
500°C Cat	--	99.57	--	92.20	--	108.88	--	80.00	--	81.72

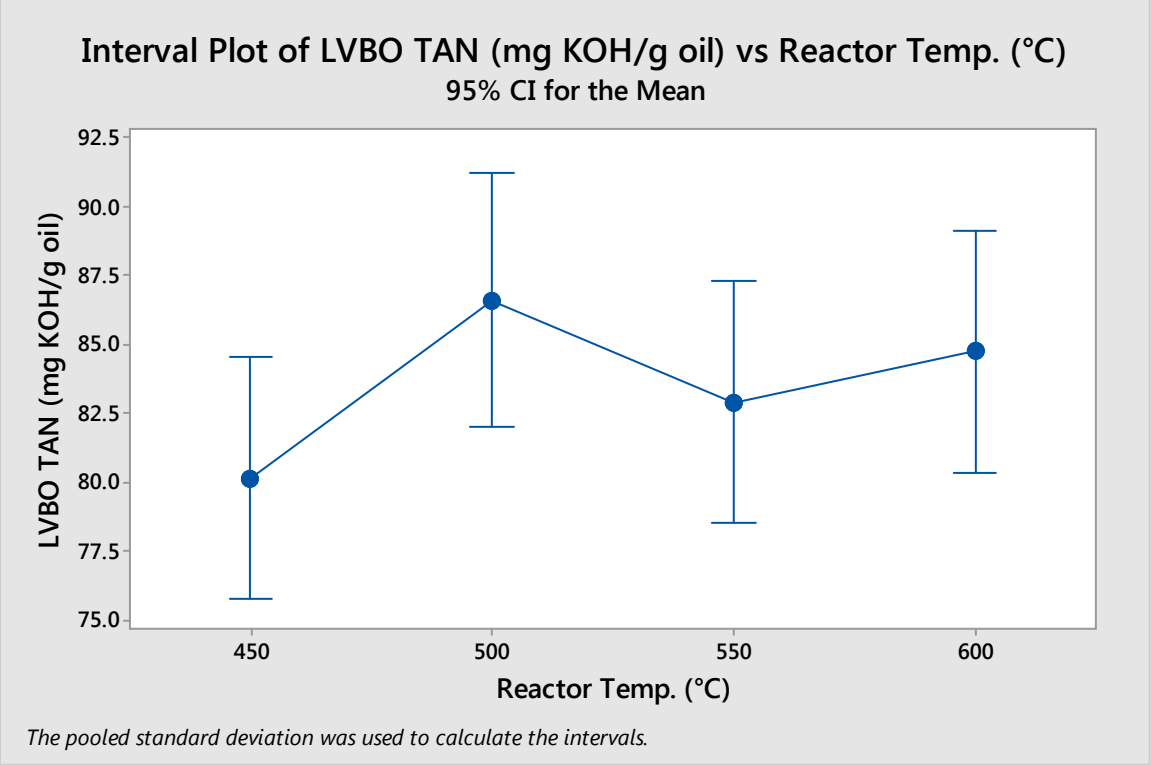

Figure 4.23: Interval Plot of LVBO TAN vs Reactor Temperature

Reactor temperature has no discernible statistically significant effect, as found by the ANOVA and Fisher tests. This could be due to the amount of noise in the data.

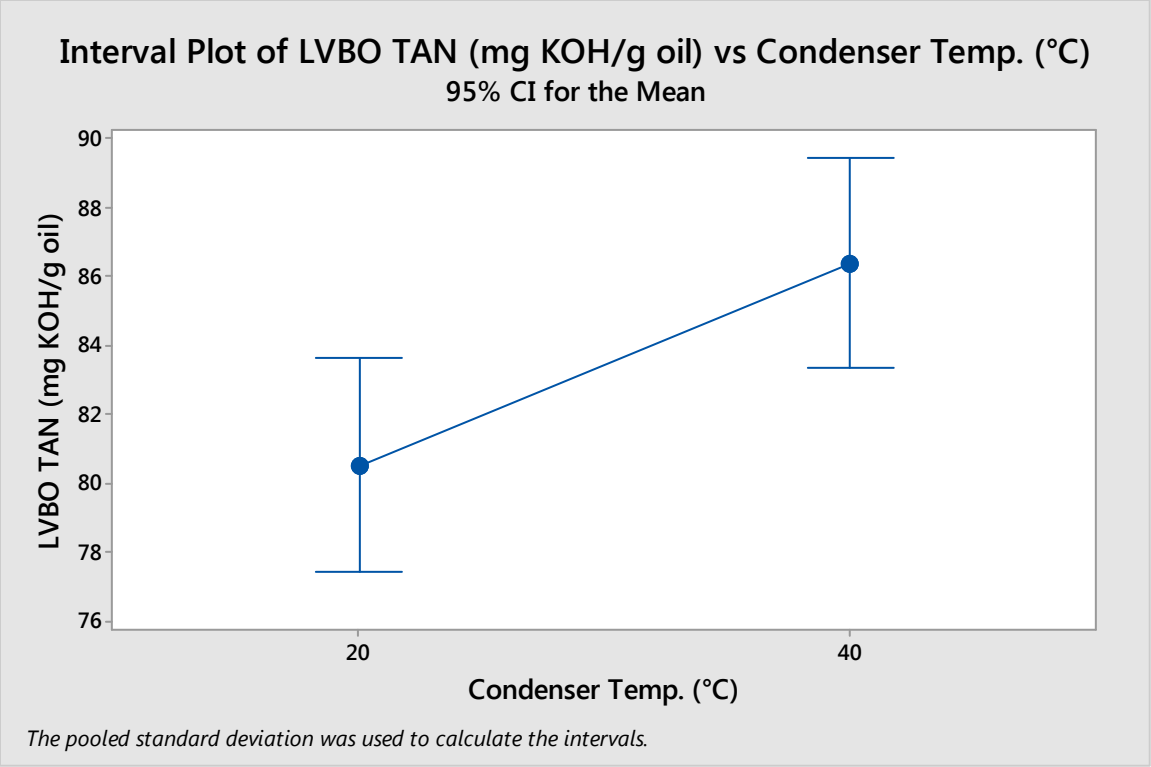

Figure 4.24: Interval Plot of LVBO TAN vs Condenser Temperature

As predicted from the table, higher condenser temperatures hold the higher TAN values (as can be seen above in Figure 4.24). The higher TAN numbers also correspond to the lower water contents, suggesting that the water could be diluting the acids at the lower temperatures. There is a slight effect of aging on the TAN; as the LVBO ages, the TAN rises slightly after one week and holds there for the remainder of the aging tests. The Fisher test once again finds that the 7-, 14-, 28-, and 84-day TAN values are not significantly different from each other, but that those four are different than the day 1 test. This is shown in Figure 4.25. However, noise levels are high enough to indicate that this could be due to the changes in procedure.

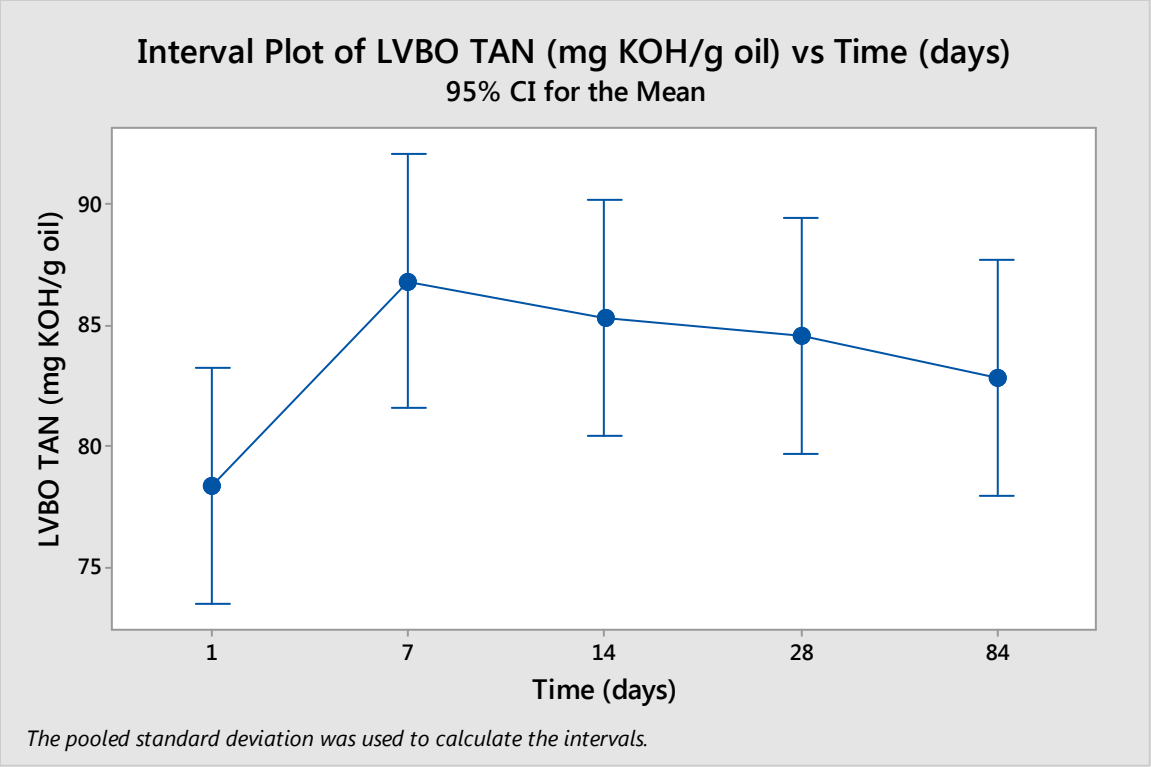

Figure 4.25: Interval Plot of LVBO TAN vs Time

4.2.5.2. HVBO TAN analysis

The TAN for the HVBO was significantly lower than the LVBO TAN, as shown in Table 4.13. The lower condenser temperatures tend to have lower TANs, which could indicate that the acids follow the water; the more water collects in the LVBO, the more acids go with it, and the fewer acids are left in the HVBO. However, some interesting fluctuations across the aging experiments suggest that there may large amounts of noise in this data as well. Small changes were made to the procedure over time in an attempt to limit the noise in the data; the standard deviation for the HVBO ended up being 4.4 mg KOH/g oil. Figure 4.26-Figure 4.28 show the interval plots for the statistical analyses.

Table 4.13: HVBO TAN

HVBO	TAN (mg KOH/g oil)									
Day	1		7		14		28		84	
Reactor Temp.	Condenser Temp.		Condenser Temp.		Condenser Temp.		Condenser Temp.		Condenser Temp.	
	20°C	**40°C**	**20°C**	**40°C**	**20°C**	**40°C**	**20°C**	**40°C**	**20°C**	**40°C**
400°C	64.84	--	--	--	--	--	--	--	--	--
450°C	20.16	18.73	17.55	21.89	18.86	21.52	19.18	19.02	12.85	21.32
500°C	15.82	24.57	19.29	20.23	13.69	24.23	18.02	26.22	21.13	32.70
550°C	14.23	24.47	15.84	19.04	17.11	20.51	19.09	22.80	20.52	27.37
600°C	17.16	14.49	18.52	19.93	14.32	20.70	16.87	18.13	19.48	26.52
500°C Cat	--	13.74	--	18.64	--	13.44	--	15.71	--	17.13

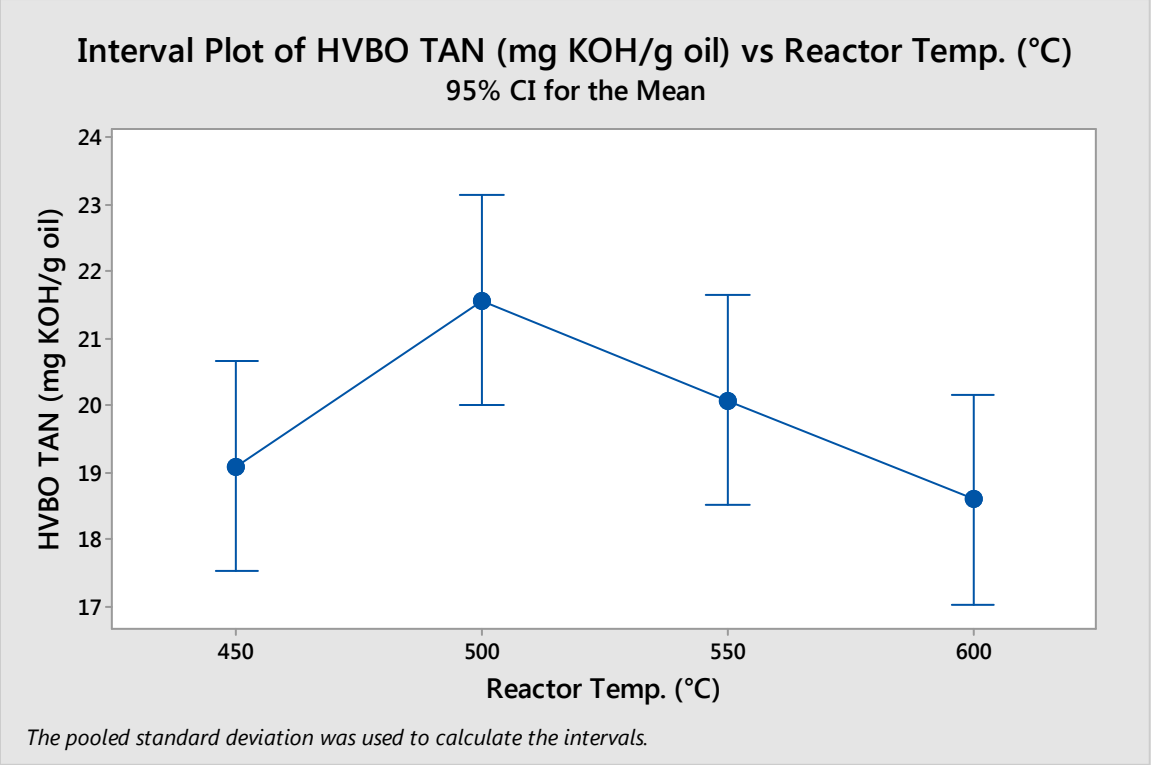

Figure 4.26: Interval Plot of HVBO TAN vs Reactor Temperature

The TAN for the 500°C reactor temperature is significantly different than the ones for 450°C, 550°C, and 600°C reactor temperatures, which in turn are not significantly

different from each other. This is likely because the 500-40 and 550-40 tests were run with a different procedure than the others; the higher values for the 550-50 were averaged with the much lower values of the 550-20, but the 500-20 was not low enough to bring the averaged 500°C reactor temperature down. This suggests that the TAN is in fact constant across the reactor temperatures; if not constant, than varying very little.

This contrasts with the condenser data below in Figure 4.27; the higher TAN corresponds to the higher condenser temperature and the higher water content from Figure 4.21. Since the first procedure run for the 500-40 and 550-40 tests gave consistently higher results than the other tests, it's likely that the difference between the two is not quite as dramatic as shown in Figure 4.21.

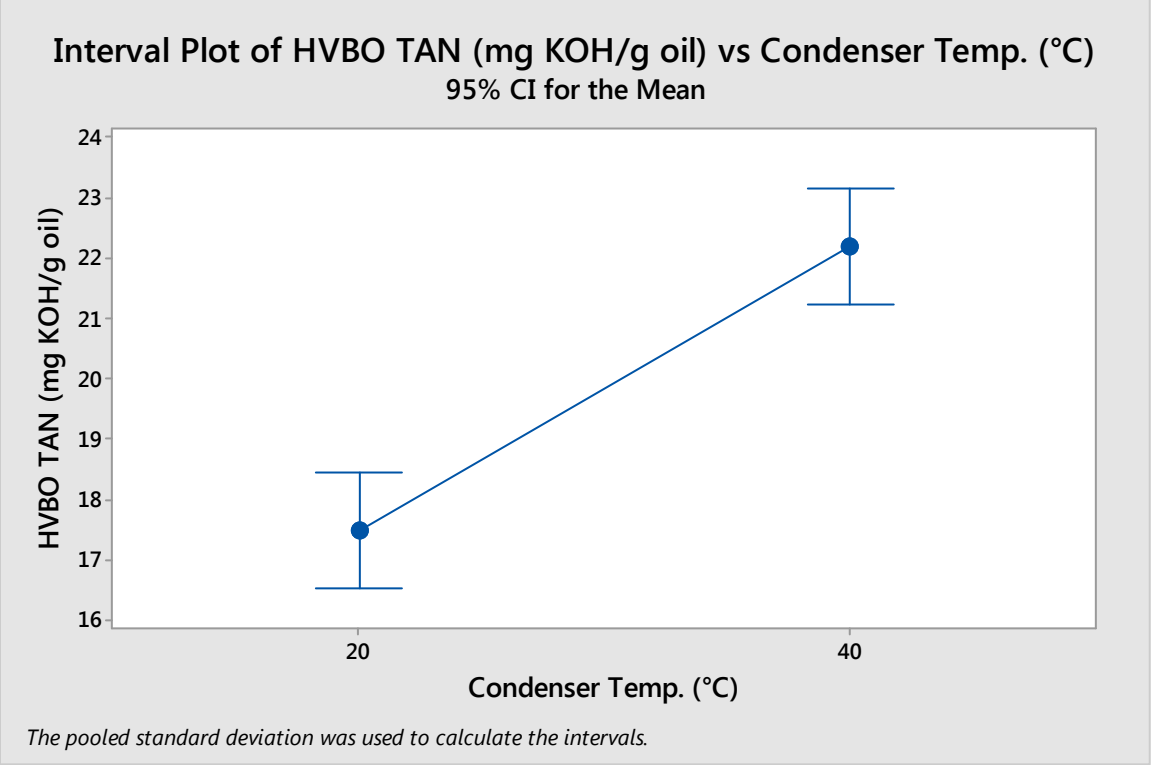

Figure 4.27: Interval Plot of HVBO TAN vs Condenser Temperature

The HVBO does not increase in TAN until it has aged for 84 days. The 1-, 7-, 14-, and 28-day tests are not significantly different from each other. However, the first procedure used gave consistently higher values for the 500-40 and 550-40 tests. Again, the difference here may not be as dramatic as shown below.

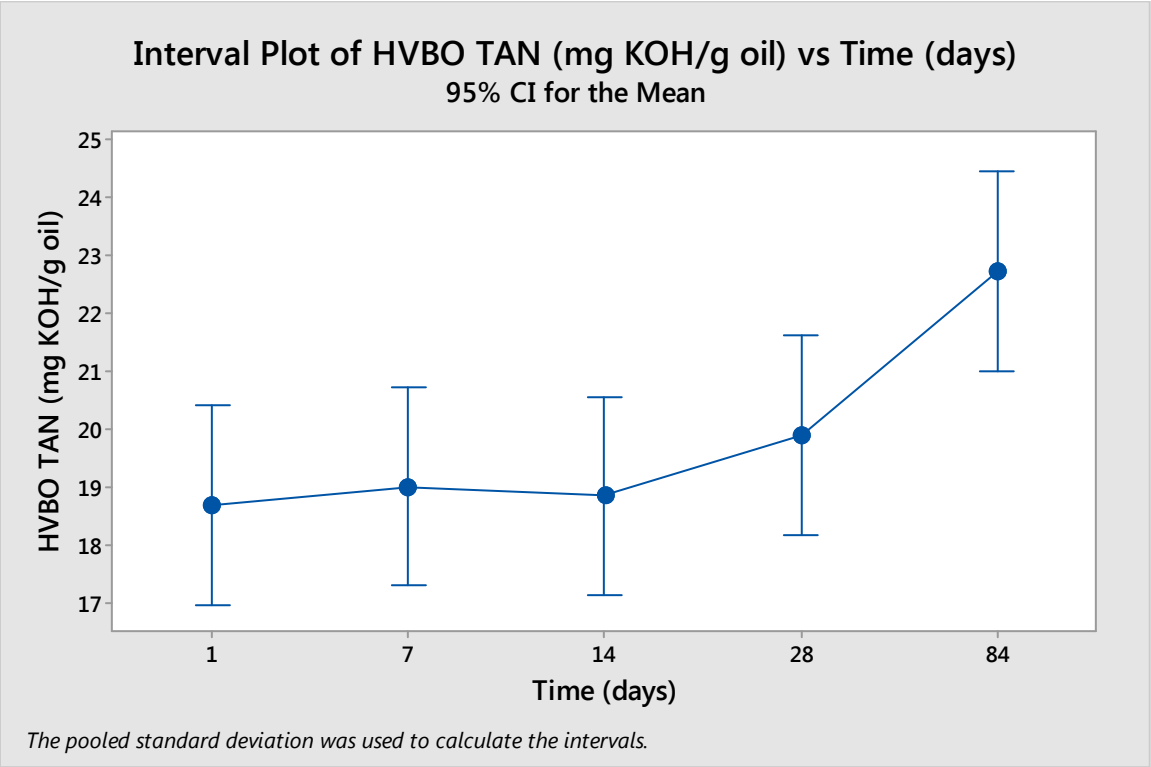

Figure 4.28: Interval Plot of HVBO TAN vs Time

4.2.6. Dynamic viscosity as a function of reactor temperature, condenser temperature, and aging

Dynamic viscosity was measured using the rheometer with the shear ramp procedure. The LVBO and HVBO were measured at all four temperatures, but the LVBO was only averaged for reporting at -5°C, 25°C, and 50°C due to boiling issues at 80°C, and HVBO was averaged for reporting at 25°C, 50°C, and 80°C due to excessive thickening at -5°C.

4.2.6.1. LVBO dynamic viscosity analysis

The dynamic viscosity of the LVBO was very low, between 0.0058 and 0.011 Pa-sec, as can be seen in Table 4.14. This could be due to the amount of water it contained. Water itself has an average viscosity across 0°C, 25°C, and 50°C of 0.0011 Pa-sec, for comparison [47]. Table 4.14 would suggest that higher viscosities exist at higher condenser temperatures, which is possible since the lower condenser temperatures contain a higher water percentage. Since each test could only be performed once due to time constraints, neither an ANOVA or a Fisher test can be run on the data, but it was graphed below in Figure 4.29.

Table 4.14: LVBO Dynamic Viscosity

LVBO	Average Dynamic Viscosity (Pa-sec)									
Day	1		7		14		28		84	
Reactor Temp.	Condenser Temp. **20°C**	**40°C**	Condenser Temp. **20°C**	**40°C**	Condenser Temp. **20°C**	**40°C**	Condenser Temp. **20°C**	**40°C**	Condenser Temp. **20°C**	**40°C**
400°C	--	--	--	--	--	--	--	--	--	--
450°C	0.0073	0.0061	0.0066	0.0059	0.0063	0.0061	0.0061	0.0058	0.0081	0.0067
500°C	0.0066	0.0064	0.0066	0.0070	0.0070	0.0072	0.0070	0.0072	0.0066	0.0096
550°C	0.0063	0.0073	0.0063	0.0079	0.0059	0.0071	0.0070	0.0074	0.0072	0.0083
600°C	0.0066	0.0072	0.0110	0.0081	0.0066	0.0071	0.0069	0.0078	0.0066	0.0085
500°C Cat	--	0.0079	--	0.0062	--	0.0063	--	0.0064	--	0.0069

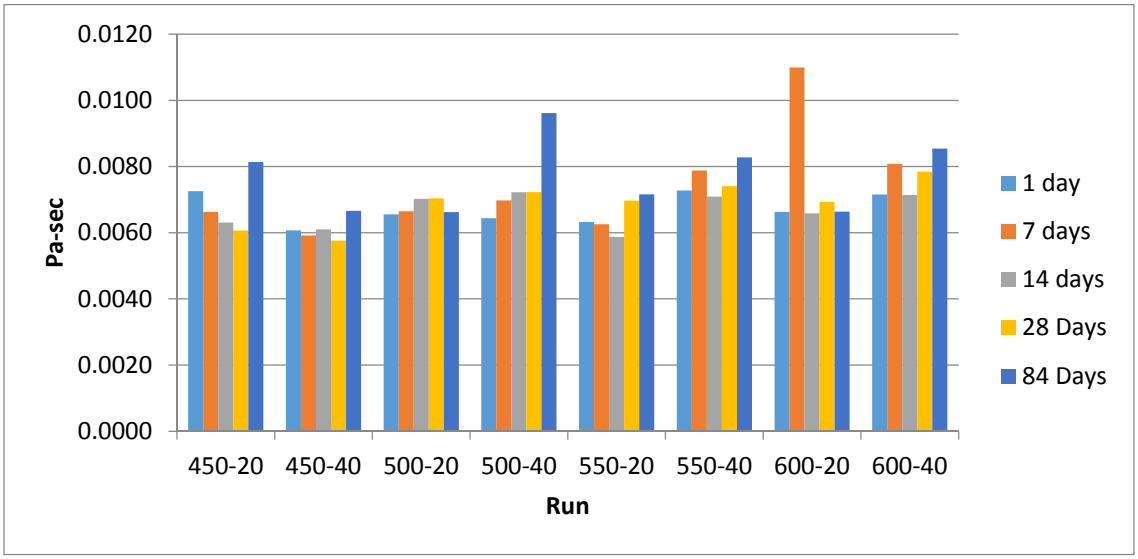

Figure 4.29: LVBO Dynamic Viscosity

There are a few outliers that can easily be identified in Figure 4.29; the 450-20 84-day test, the 500-40 84-day test, and the 600-20 7-day test are likely the results of bad experiments due to human error. Condenser temperatures have a slight effect on viscosity, tending to be slightly higher at the higher condenser temperatures. Higher reactor temperatures also contribute to slightly higher viscosities. No real difference for the aging experiments can readily be seen.

4.2.6.2. HVBO dynamic viscosity analysis

There is a clearly discernible trend in Table 4.15 regarding the HVBO; the lower condenser temperatures have lower viscosities. This cannot be linked to water, since the water content is in fact lower at the lower condenser temperatures, but it could be linked to low-viscosity volatiles condensing in the HVBO that contribute to both the energy content and the viscosity. In addition, the viscosity increases with increasing reactor temperature.

The high outliers at 600-40 84-day test and 500-40CAT 84-day test can be explained by a short-lived experiment to aid syringe flow; the two oil samples were heated in an 80°C water bath. This aided flow into the syringe initially but ultimately increased the viscosity as some water and/or volatiles evaporated. There could have been additional human error involved during the measurement phase as well, since the viscosity was almost a full order of magnitude higher than the preceding experiments for both 600-40 and 500-40Cat.

As Table 4.15 also shows, the higher reactor temperatures also have higher viscosities. Aging data is also shown in Figure 4.30.

Table 4.15: HVBO Dynamic Viscosity

HVBO	Average Dynamic Viscosity (Pa-sec)									
Day	1		7		14		28		84	
Reactor Temp.	Condenser Temp.		Condenser Temp.		Condenser Temp.		Condenser Temp.		Condenser Temp.	
	20°C	**40°C**	**20°C**	**40°C**	**20°C**	**40°C**	**20°C**	**40°C**	**20°C**	**40°C**
400°C	0.49	--	--	--	--	--	--	--	--	--
450°C	0.40	0.86	0.63	1.27	0.50	1.67	0.93	1.94	1.67	2.74
500°C	0.36	0.94	0.84	1.50	1.10	3.63	2.30	3.53	1.22	1.15
550°C	0.36	0.93	0.89	2.10	1.57	2.51	3.60	3.10	1.35	3.75
600°C	0.48	1.45	1.02	0.98	1.13	1.06	1.58	1.30	1.60	7.82
500°C Cat	--	0.72	--	1.42	--	1.84	--	3.12	--	7.24

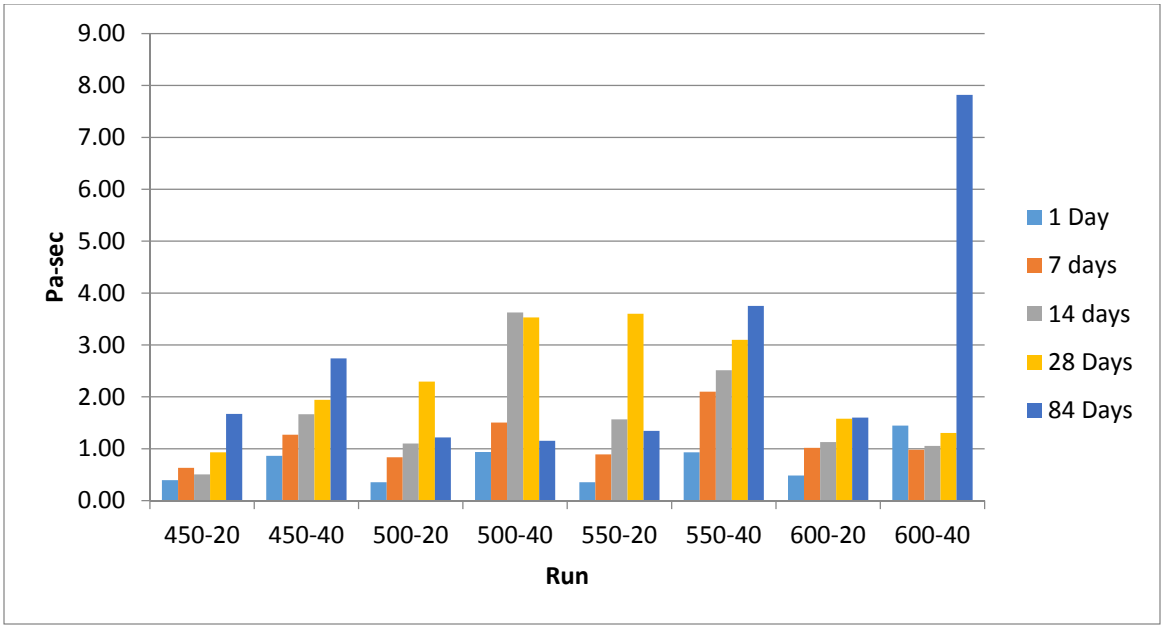

Figure 4.30: HVBO Dynamic Viscosity

As Figure 4.30 shows, there is a general increase in dynamic viscosity as the oil ages. This increase in viscosity could be due to changes in chemical compounds; the reduction of carbonyl, aldehydes, ketones and carboxylic acids as the phenolic compounds increased is one potential mechanism [25]. The HVBO also tends to separate from any water that it may contain, causing water pockets to become trapped in the oil. The low points at 500-20, 500-40, 550-40, and 600-20 were caused by water separation in the viscometer. The viscous HVBO clung to the upper plate and "slid," to a certain extent, on the water that settled below it. This effect was the most pronounced at -5°C and 25°C. As the HVBO rose in temperature, it became less viscous and reabsorbed the water.

4.2.7. Catalyst comparison

In order to perform a catalyst comparison, zeolite catalyst was mixed with the usual 1.5 kg of biomass in a 10:1 biomass/catalyst and fed through the auger reactor. As shown in Figure 19 in the Yield Analysis section, the catalyst run yielded less HVBO and LVBO than the 500-40 run without the catalyst. However, it did recover more total mass since the char recovery was large.

As can be seen in Table 4.16, The LVBO catalyst-aided bio-oil was consistently lower than its counterpart in energy content and viscosity and consistently higher in water content. The TAN was difficult to measure, but it averaged higher for the catalyst runs. There were no significant aging effects that differed between the 500-40 and the 500-40Cat runs for LVBO.

Table 4.16: LVBO Catalyst Comparison

LVBO	Catalyst Comparison				
Day	1	7	14	28	84
Reactor Temp.	Condenser Temperature				
	40°C	**40°C**	**40°C**	**40°C**	**40°C**
	Energy Content (kJ/kg)				
500°C	8404	8262	8142	8245	8281
500°C CAT	8064	7785	7790	7660	8013
	Water Content (% H2O)				
500°C	60.09	60.55	58.58	60.62	62.48
500°C CAT	61.98	61.36	57.38	64.02	62.12
	TAN (mg KOH/g oil)				
500°C	59.40	106.42	93.22	90.64	79.13
500°C CAT	99.57	92.20	108.88	80.00	81.72
	Average Dynamic Viscosity (Pa-sec)				
500°C	0.0064	0.0070	0.0072	0.0072	0.0096
500°C CAT	0.0079	0.0062	0.0063	0.0064	0.0069

For the HVBO catalyst comparison, the energy content is higher and the water content, TAN, and viscosity are all lower for the experimental run with catalyst. No significant aging differences are evident in the energy content or water content, while the catalyst-aided HVBO has a significantly lower TAN and less of a TAN rise as it aged. A similar situation happened with viscosity until the 84-day test and the outlier in the 500-40Cat viscosity; this was the result of a heating experiment, as previously mentioned.

Table 4.17: HVBO Catalyst Comparison

HVBO	Catalyst Comparison				
Day	1	7	14	28	84
Reactor Temp.	Condenser Temperature				
	40°C	**40°C**	**40°C**	**40°C**	**40°C**
	Energy Content (kJ/kg)				
500°C	27155	26886	27281	27944	28259
500°C CAT	27651	27584	28607	28701	28777
	Water Content (% H2O)				
500°C	12.24	12.52	13.00	11.54	12.22
500°C CAT	12.48	12.06	12.05	10.77	12.31
	TAN (mg KOH/g oil)				
500°C	24.57	20.23	24.23	26.22	32.70
500°C CAT	13.74	18.64	13.44	15.71	17.13
	Average Dynamic Viscosity (Pa-sec)				
500°C	0.94	1.50	3.63	3.53	1.15
500°C CAT	0.72	1.42	1.84	3.12	7.24

4.2.8. Usable energy yield versus operating conditions

While the calorific values are higher at 450-20 than any other point taken, the actual usable energy yield, as defined as the energy content per kilogram of input biomass. This was found by multiplying the energy content by the mass fraction. Table 4.18 shows the comparison for the HVBO.

Table 4.18: Usable Energy Content versus Reactor and Condenser Temperature

Usable Energy (MJ/kg biomass input)		
Species	HVBO	
Reactor Temp (°C)	Condenser Temp (°C)	
	20	**40**
400	0.95	--
450	2.66	3.81
500	3.13	5.50
550	3.43	4.90
600	5.09	5.54
500 CAT	--	3.44

As can be seen, the best return can be found at the 600-40 reactor-condenser temperature conditions. This indicates that, between the oil yield and oil properties, this is the best return for the input.

CHAPTER 5: CONCLUSIONS AND FUTURE WORK

5.1. Conclusions

The investigation of bio-oil produced from carinata meal through fast pyrolysis was accomplished by varying the reactor temperature between 450°C, 500°C, 550°C, and 600°C and the condenser temperature between 20°C and 40°C. The yield, energy content, water content, TAN, and dynamic viscosity were then measured. The latter four measurements were repeated after 7, 14, 28, and 84 days to determine the effects of aging on the bio-oil. Two types of oil were collected, LVBO and HVBO.

The LVBO has lower energy content, higher water content, higher TAN, and lower viscosity than the HVBO. There is almost no aging effects that can be seen for the LVBO. The best oil, as characterized by high energy content, low viscosity, low TAN, low water content, and minimal aging, is the HVBO at 450-20 reactor/condenser conditions. The best return, as characterized by the energy content per kilogram of processed biomass, is at the 600-40 reactor/condenser temperature.

Oil yield is lower than predicted, due to auger configuration; while lower auger speeds give more oil yield, the auger jams at slow speeds. This is due to either auger damage, uneven thermal expansion, or char buildup.

5.1.1. Effects of reactor temperature

For the LVBO, the yield is roughly the same across the temperatures, with a mass fraction ranging between 19% and 22%. For the yield repeatability of the reactor, these mass fractions are statistically identical. The energy content is maximum at 500°C, 550°C, and 600°C, hovering around 8.1 MJ/kg. The oils for these three reactor

temperatures are not statistically significantly different from each other. The lowest energy content occurred with a reactor temperature of 450°C, at 7.7 MJ/kg.

In addition, the water content declines slowly but steadily with increasing reactor temperature for LVBO, going from an average of 64% at 450°C to 60% at 600°C. The TAN for LVBO averages at 82.5 mg KOH/g oil, with no statistically significant difference between the four reactor temperatures. Viscosity rises with increasing reactor temperatures. Values for viscousity tend to be near 0.007 Pa-sec.

For HVBO, the yield is higher with higher reactor temperatures—since more of the biomass can go through pyrolysis faster, this makes sense. The yield ranges between 9% to 20% mass fraction. The energy content is maximum at 450°C reactor temperature, with an average value of 29.3 MJ/kg. The energy content then drops to an average value of 27.8 MJ/kg when the reactor is set to 500°C, 550°C, or 600°C. Water content rises with rising reactor temperature, suggesting hydrogen cracking is occurring during pyrolysis and forming water. This would account for the lower energy contents at the higher reactor temperatures as well. The lowest water content is 10.25% at 450°C, while 500°C, 550°C, and 600°C hover around 12%.

HVBO TAN ranges from 18.75 mg KOH/g oil and 22 mg KOH/g oil. The highest TAN (22 mg KOH/g oil) is at a 500°C reactor temperature. The other three temperatures are not significantly different from each other. The viscosity rises with higher reactor temperature, until the 600°C temperature, which has a similar viscosity as the 450°C reactor temperature.

5.1.2. Effects of condenser temperature

Higher yields of LVBO are collected at lower condenser temperatures, indicating that more water and possibly volatiles are being condensed. The energy content is lower at the 20°C condenser temperatures (7.7 MJ/kg as opposed to 8.1 MJ/kg), which indicates that it is predominately extra water that is being condensed and collected. The water content confirms this; the water content at 20°C averages to be 64%, as opposed to the 60.5% average at 40°C. The TAN is higher at 40°C; at an average of 87 mg KOH/g oil, it is a bit higher than the 20°C 80.5 mg KOH/g oil. Viscosity rises slightly with higher condenser temperatures for LVBO.

HVBO condenser effects are almost completely opposite the LVBO effect. Yields are higher at higher condenser temperatures, hovering around 20% mass fraction collection for the 40°C condenser temperature, while the 20°C condenser temperature ranges from 9% to 18%. Lower energy contents of 27.85 MJ/kg were collected at 40°C, while higher energy contents averaging at 28.7 MJ/kg were collected from the 20°C condenser temperature. This corresponds to the lower water content (average 11.2%) collected from 20°C and the higher water content collected at 40°C, which averaged 12.2%. There was a much lower TAN at 20°C versus 40°C: 17.25 mg KOH/g oil versus 22.2 mg KOH/g oil. The viscosities were also lower at 20°C versus the 40°C, although the differences weren't as pronounced; 0.5 Pa-sec versus 1.1 Pa-sec for the day 1 tests.

5.1.3. Aging effects on the oil properties

Aging has no effect on the LVBO energy content, water content, or viscosity. There is a slight increase in TAN, rising from an average of 78 mg KOH/g oil to 85 mg

KOH/g oil that happens from day 1 to day 7, after which changes are statistically insignificant.

Aging has a slight effect on energy content and water content for HVBO. The energy content rises from 27.5 MJ/kg to 28.5MJ/kg average, while the water content drops from an average of 13% to 11%. The TAN remains constant at 18.5 mg KOH/g oil until the final test at 84 days, when it increases to 23.5 mg KOH/g oil. The viscosity shows the most dramatic change; it changes steadily, going from an average of 0.8 Pa-sec to 2.65 Pa-sec. Some samples show increases in excess of 3.0 Pa-sec.

5.1.4. Catalyst effects

The LVBO catalyst run had a slightly higher water content and significantly higher TAN than the LVBO without the catalyst (61% and 92.4 mg KOH/g oil versus 60% and 86 mg KOH/g oil). The LVBO catalyst run also had a lower energy content of 7.9 MJ/kg as opposed to the regular LVBO run at 8.3 MJ/kg. The viscosity for the LVBO catalyst run was also lower, at 0.0068 Pa-sec compared to 0.0075 Pa-sec. The aging effects for both were similar and followed the same trends previously seen for LVBO.

The HVBO catalyst run was different. It had a higher energy content (28.3 MJ/kg versus 27.5 MJ/kg), a lower water content (11.9% as opposed to 12.3%), and a lower TAN (15.73 mg KOH/g oil compared to 25.59 mg KOH/g oil). Once adjusted to remove the unusually high 84-day viscosity test for the 500-20CAT run (due to a combination of excessive preheating and human error during testing), the viscosity for the catalyst run was also lower, at 1.77 Pa-sec versus 2.15 Pa-sec for the non-catalyst HVBO. The aging effects were lower for the catalyst run than they were for the non-catalyst run; the water

content remained fairly constant, the energy content increased a little, and the viscosity only increased from 0.72 to 3.12 Pa-sec, as opposed to the 0.94 to 3.53 Pa-sec increase in the non-catalyst HVBO.

5.2. Future work

Elemental analysis should be made for future aging tests to determine exactly what changes happen in the HVBO over the course of the aging process. This is especially important with regards to the viscosity—the viscosity increases greatly, but the exact mechanism is unknown. This analysis might also shed more light on why the carinata oil separates into the two oil components during the pyrolysis process.

In addition, the carbon, hydrogen, nitrogen, and oxygen quantities in the oil should be measured with a CHNS-O analyzer in order to get an idea of the components in the oil and their relative quantities.

First and foremost, each run should be performed a few more times to get repeatability for the entire test, as well as to get repeatability data for yield and viscosity. Elemental analysis and mass spectroscopy should both be utilized to pinpoint the exact nature of the changes in viscosity during the aging processes of the oil. The auger reactor should also be scrutinized for any enhancements that could aid in making yield more precise.

The auger needs to be examined to find the root cause of the jams. If thermal expansion is the root cause, the insulation needs to be reworked so the heating is uniform across the reactor. If the auger is damaged, it needs to be replaced. If char buildup is the

issue, the motor either needs to be replaced with one that can deliver more torque or the reactor needs to be lengthened.

A few more catalyst runs should be made, at least one at the 450-20 reactor/condenser conditions, in order to compare the catalyst against the best conditions for HVBO quality.

REFERENCES

[1] Perlack, R. D., Wright, L. L., Turhollow, A. F., Graham, R. L., Stokes, B. J. E., and Erbach, D. C., 2005, "Biomass as feedstock for a bioenergy and bioproducts industry: the technical feasibility of a billion-ton annual supply," DTIC Document, p. 78.

[2] Yu, P., Xin, H., Ban, Y., and Zhang, X., 2014, "Interactive association between biopolymers and biofunctions in carinata seeds as energy feedstock and their coproducts (carinata meal) from biofuel and bio-oil processing before and after biodegradation: current advanced molecular spectroscopic investigations," Journal of Agricultural and Food Chemistry, 62(18), pp. 4039-4047.

[3] Xin, H., Falk, K. C., and Yu, P., 2013, "Studies on brassica carinata seed. 1. Protein molecular structure in relation to protein nutritive values and metabolic characteristics," Journal of Agricultural and Food Chemistry, 61(42), pp. 10118-10126.

[4] Bellostas, N., Sørensen, J., and Sørensen, H., 2004, "Qualitative and quantitative evaluation of glucosinolates in cruciferous plants during their life cycles," Agroindustria, 3(3), p. 5.

[5] Alexander, J., Auðunsson, G. A., Benford, D., Cockburn, A., Cravedi, J.-P., Dogliotti, E., Di Domenico, A., Férnandez-Cruz, M. L., Fürst, P., Fink-Gremmels, J., Galli, C. L., Grandjean, P., Gzyl, J., Heinemeyer, G., Johansson, N., Mutti, A., Schlatter, J., Van Leeuwen, R., Van Peteghem, C., and Verger, P., 2008, "Glucosinolates as undesirable substances in animal feed; scientific panel on contaminants in the food chain," The EFSA Journal, 590, pp. 1-76.

[6] Cardone, M., Mazzoncini, M., Menini, S., Rocco, V., Senatore, A., Seggiani, M., and Vitolo, S., 2003, "Brassica carinata as an alternative oil crop for the production of

biodiesel in Italy: agronomic evaluation, fuel production by transesterification and characterization," Biomass & Bioenergy, 25(6), pp. 623-636.

[7] Xin, H., Falk, K. C., and Yu, P., 2013, "Studies on brassica carinata seed. 2. Carbohydrate molecular structure in relation to carbohydrate chemical profile, energy values, and biodegradation characteristics," Journal of Agricultural and Food Chemistry, 61(42), pp. 10127-10134.

[8] Bouaid, A., Martinez, M., and Aracil, J., 2009, "Production of biodiesel from bioethanol and Brassica carinata oil: oxidation stability study," Bioresource Technology, 100(7), pp. 2234-2239.

[9] Bouaid, A., Diaz, Y., Martinez, M., and Aracil, J., 2005, "Pilot plant studies of biodiesel production using brassica carinata as raw material," Catalysis Today, 106(1-4), pp. 193-196.

[10] Coppola, E. N., and Red, C., 2011, "Renewable, Aromatic, Drop-in (Readi) Fuels," Applied Research Associates, p. 2.

[11] Newlands, N. K., Townley-Smith, L., and Porcelli, T. A., 2012, "A renewable source of jetfuel from alternative oilseeds? Predicting crop response under environmental variability," Agriculture and Agri-Food.

[12] Bridgwater, A. V., Carson, P., and Coulson, M., 2007, "A comparison of fast and slow pyrolysis liquids from mallee " International Journal of Global Energy Issues, Vol. 27(No. 2), pp. 204-216.

[13] Sohi, S. P., Krull, E., Lopez-Capel, E., and Bol, R., 2010, "A review of biochar and its use and function in soil," Advances in Agronomy, pp. 47-82.

[14] Clough, T. J., and Condron, L. M., 2010, "Biochar and the nitrogen cycle: introduction," Journal of Environment Quality, 39(4), p. 1218.

[15] Harris, J., Lawburgh, J., Lawburgh, B., Michna, G. J., and Gent, S. P., 2014, "Properties of brassica carinata and camelina sativa meals and fast pyrolysis derived bio-oils," 12th Fuel Cell, Science Engineering and Technology Conference p. 6.

[16] Bridgwater, A. V., 2007, "The production of biofuels and renewable chemicals by fast pyrolysis of biomass " International Journal of Global Energy Issues, Vol. 27(No. 2), pp. 160-203.

[17] Bridgwater, A. V., 2012, "Review of fast pyrolysis of biomass and product upgrading," Biomass & Bioenergy, 38, pp. 68-94.

[18] Brown, R. C., 2003, *Biorenewable Resources—Engineering New Products from Agriculture*, Iowa State Press, Ames, IA.

[19] Mullen, C. A., Boateng, A. A., Goldberg, N. M., Lima, I. M., Laird, D. A., and Hicks, K. B., 2010, "Bio-oil and bio-char production from corn cobs and stover by fast pyrolysis," Biomass and Bioenergy, 34(1), pp. 67-74.

[20] Green, A. E. S., and Feng, J., 2006, "Systematics of corn stover pyrolysis yields and comparisons of analytical and kinetic representations," Journal of Analytical and Applied Pyrolysis, 76(1-2), pp. 60-69.

[21] Czernik, S., and Bridgwater, A. V., 2004, "Overview of applications of biomass fast pyrolysis oil," Energy & Fuels, 18(2), pp. 590-598.

[22] Shen, J., Wang, X.-S., Garcia-Perez, M., Mourant, D., Rhodes, M. J., and Li, C.-Z., 2008, "Effects of particle size on the fast pyrolysis of oil mallee woody biomass," Elesevier, Fuel(88), pp. 1810-1817.

[23] Bridgeman, T. G., Darvell, L. I., Jones, J. M., Williams, P. T., Fahmi, R., Bridgwater, A. V., Barraclough, T., Shield, I., Yates, N., Thain, S. C., and Donnison, I. S., 2007, "Influence of particle size on the analytical and chemical properties of two energy crops," Fuel, 86(1-2), pp. 60-72.

[24] Alcala, A., and Bridgwater, A. V., 2013, "Upgrading fast pyrolysis liquids: Blends of biodiesel and pyrolysis oil," Fuel, 109, pp. 417-426.

[25] Grioui, N., Halouani, K., and Agblevor, F. A., 2014, "Bio-oil from pyrolysis of tunisian almond shell: Comparative study and investigation of aging effect during long storage," Energy for Sustainable Development, 21, pp. 100-112.

[26] Garcia-Perez, M., Wang, X. S., Shen, J., Rhodes, M. J., Tian, F. J., Lee, W. J., Wu, H. W., and Li, C. Z., 2008, "Fast pyrolysis of oil mallee woody biomass: Effect of temperature on the yield and quality of pyrolysis products," Ind Eng Chem Res, 47(6), pp. 1846-1854.

[27] Garcia-Perez, M., Shen, J., Wang, X. S., and Li, C. Z., 2010, "Production and fuel properties of fast pyrolysis oil/bio-diesel blends," Fuel Processing Technology, 91(3), pp. 296-305.

[28] Hilten, R. N., and Das, K. C., 2010, "Comparison of three accelerated aging procedures to assess bio-oil stability," Fuel, 89(10), pp. 2741-2749.

[29] Kimura, L. M., Santos, L. C., Vieira, P. F., Parreira, P. M., and Henrique, H. M., 2010, "Biomass pyrolysis: use of some agricultural wastes for alternative fuel production," Materials Science Forum, 660-661, pp. 259-264.

[30] Badger, P. C., and Fransham, P., 2006, "Use of mobile fast pyrolysis plants to densify biomass and reduce biomass handling costs—A preliminary assessment," Biomass and Bioenergy, 30(4), pp. 321-325.

[31] Bridgwater, A. V., Toft, A. J., and Brammer, J. G., 2002, "A techno-economic comparison of power production by biomass fast pyrolysis with gasification and combustion," Renew Sust Energ Rev, 6(3), pp. 181-248.

[32] Milazzo, M. F., Spina, F., Vinci, A., Espro, C., and Bart, J. C. J., 2013, "Brassica biodiesels: Past, present and future," Renew Sust Energ Rev, 18, pp. 350-389.

[33] Qu, W., Wei, L., Ma, Z., and Julson, J., 2012, "Fast pyrolysis of corn stover and sawdust in a novel reactor," Proceedings of the ASABE Annual International Meeting.

[34] Jiang, G. Z., Nowakowski, D. J., and Bridgwater, A. V., 2010, "A systematic study of the kinetics of lignin pyrolysis," Thermochim Acta, 498(1-2), pp. 61-66.

[35] Gani, A., and Naruse, I., 2007, "Effect of cellulose and lignin content on pyrolysis and combustion characteristics for several types of biomass," Renew Energ, 32(4), pp. 649-661.

[36] Pittman, C. U., Mohan, D., Eseyin, A., Li, Q., Ingram, L., Hassan, E.-B. M., Mitchell, B., Guo, H., and Steele, P. H., 2012, "Characterization of bio-oils produced from fast pyrolysis of corn stalks in an auger reactor," Energy & Fuels, 26(6), pp. 3816-3825.

[37] Ingram, L., Mohan, D., Bricka, M., Steele, P., Strobel, D., Crocker, D., Mitchell, B., Mohammad, J., Cantrell, K., and Pittman, C. U., 2008, "Pyrolysis of wood and bark in an auger reactor: physical properties and chemical analysis of the produced bio-oils," Energy & Fuels, 22(1), pp. 614-625.

[38] Lu, Q., Li, W.-Z., and Zhu, X.-F., 2009, "Overview of fuel properties of biomass fast pyrolysis oils," Energy Conversion and Management, 50(5), pp. 1376-1383.

[39] Mihalcik, D. J., Mullen, C. A., and Boateng, A. A., 2011, "Screening acidic zeolites for catalytic fast pyrolysis of biomass and its components," Journal of Analytical and Applied Pyrolysis, 92(1), pp. 224-232.

[40] Yildiz, G., Pronk, M., Djokic, M., van Geem, K. M., Ronsse, F., van Duren, R., and Prins, W., 2013, "Validation of a new set-up for continuous catalytic fast pyrolysis of biomass coupled with vapour phase upgrading," Journal of Analytical and Applied Pyrolysis, 103, pp. 343-351.

[41] Yildiz, G., Lathouwers, T., Toraman, H. E., van Geem, K. M., Marin, G. B., Ronsse, F., van Duren, R., Kersten, S. R. A., and Prins, W., 2014, "Catalytic fast pyrolysis of pine wood: Effect of successive catalyst regeneration," Energy & Fuels, 28(7), pp. 4560-4572.

[42] Bridgwater, A. V., and Peacocke, G. V. C., 2000, "Fast pyrolysis processes for biomass," Renew Sust Energ Rev, 4(1), pp. 1-73.

[43] Xiong, Q. G., Aramideh, S., and Kong, S. C., 2013, "Modeling effects of operating conditions on biomass fast pyrolysis in bubbling fluidized bed reactors," Energy & Fuels, 27(10), pp. 5948-5956.

[44] IKA, 2007, "IKA calorimeter system operating instructions," IKA.

[45] Instruments, T., 2007, AR 2000 Rheometer, rheometrics series operator's manual.

[46] Gas, M., Accessed 01/19/2015, "Basic flowmeter principes," Flow Measurement and Control: Rotometers, p. 4.

[47] Munson, B. R., Young, D. F., Okiishi, T. H., and Huebsch, W. W., 2009, *Fundamentals of Fluid Mechanics*, Don Fowley.